Zeitschrift: IABSE congress report = Rapport du congrès AIPC = IVBH Kongressbericht

Band: 12 (1984)

Rubrik: V. Developments in the design of steel structures

SEMINAR

V

Developments in the Design of Steel Structures

Développements dans le projet et le calcul de constructions métalliques

Fortschritte in Entwurf und Berechnung von Stahltragwerken

Chairman: Li Guohao, China

Coordinator: J.C. Badoux, Switzerland

General Reporter: G. Sedlacek, Fed. Rep. of Germany

The theme has been introduced by the General Reporter in the Introductory Report of the 12th Congress, available at the IABSE Secretariat.

Leere Seite
Blank page
Page vide

Strength of Longitudinal and Cross Girders of Steel Railway Bridges

Résistance des longerons et entretoises de ponts-rails métalliques

Festigkeit der Längs- und Querträger stählerner Eisenbahnbrücken

Marcel A. TSCHUMI
Civil Engineer
Swiss Federal Railways
Berne, Switzerland

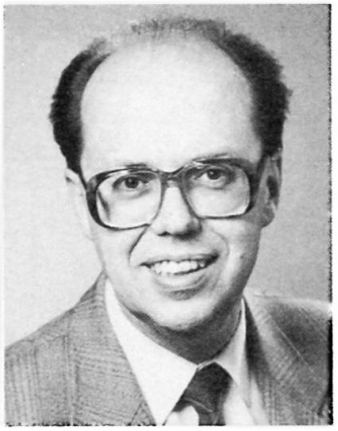

Marcel A. Tschumi, born 1938, obtained his civil engineering diploma at the Swiss Federal Institute of Technology in Zürich in 1962. Since then he has been involved in the design of structures and bridges.

SUMMARY

The present paper gives details of the organisation and execution of strain gauge tests on longitudinal and cross girders on five different European single track steel railway bridges. The bridges were subjected to known static and dynamic loads (test locomotives) and to about 100 service trains the wheel loads of which were measured. The work is a joint effort of the Office for Research and Experiments of the International Union of Railways.

RESUME

L'article donne quelques détails sur l'organisation et l'exécution de mesures extensométriques sur les longerons et entretoises de ponts métalliques à voie unique, situés dans cinq pays européens. Les ponts ont été soumis à des charges statiques et dynamiques définies (locomotives test) ainsi qu'au passage d'environ 100 trains de service dont les charges par roue avaient été mesurées. Il s'agit d'un travail exécuté au sein de l'Office de Recherches et d'Essais de l'Union Internationale des Chemins de Fers.

ZUSAMMENFASSUNG

Der vorliegende Artikel gibt einige Angaben über die Organisation und die Durchführung von Dehnungsmessungen an Längs- und Querträgern von fünf einspurigen, stählernen Eisenbahnbrücken in Europa. Die Brücken wurden bekannten statischen und dynamischen Belastungen ausgesetzt (Versuchslokomotiven) sowie rund 100 Betriebszügen, von denen die Radlasten gemessen worden sind. Es handelt sich um eine Gemeinschaftsarbeit des Forschungs- und Versuchsamt des Internationalen Eisenbahnverbandes.

1. INTRODUCTION

Five steel single track truss bridges with rail bearers and cross girders were tested. These belong to the railways CFR (Rumania), PKP (Poland), NS (Netherlands), SBB (Switzerland) and JŽ (Jugoslavia). They were chosen to cover a wide range of cross girder spacings (3.875m to 9.55m). The most important data of the bridge decks are the following:

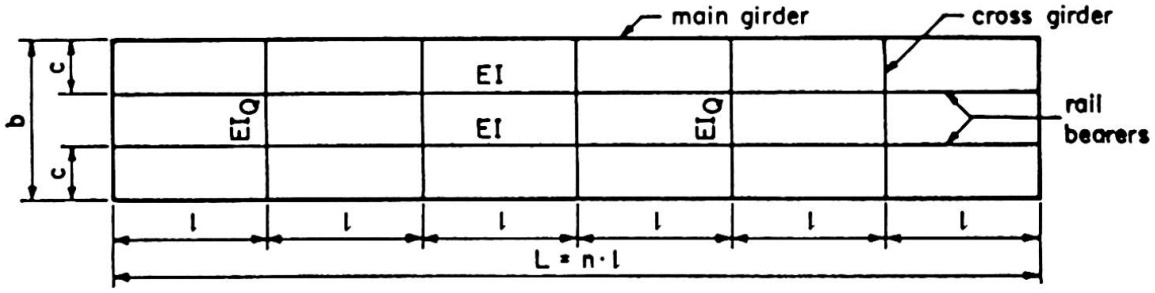

rail-way	main span L (m)	n	rail bearers l (m)	rail bearers I (m^4)	cross girders b (m)	cross girders c (m)	cross girders I_Q (m^4)
CFR	31.00	8	3.875	0.399×10^{-3}	5.00	1.60	2.26×10^{-3}
PKP	55.10	10	5.510	2.609×10^{-3}	5.10	1.65	6.77×10^{-3}
NS	59.64	12	4.970	0.842×10^{-3}	5.12	1.79	2.28×10^{-3}
SBB	65.80	10	6.580	2.122×10^{-3}	5.00	1.65	6.54×10^{-3}
JŽ	95.50	10	9.550	6.954×10^{-3}	5.80	2.00	9.31×10^{-3}

Fig. 1 Data of bridge deck

All five railways took their measurements on riveted bridges, and in all bridges, rail bearer continuity is achieved by means of continuity plates and fastenings.

The object of the measurements was to establish, for rail bearers and cross girders:

- a more realistic method of static design calculation
- better knowledge of the dynamic increment caused by railway loading
- the load spectra for fatigue calculations

To achieve this object it was necessary to measure:

- the wheel loads and axle spacing for the test train and service traffic
- the magnitude of the static forces on the rail bearers and cross girders produced by the test train
- the magnitude of the dynamic forces on the rail bearers and cross girders produced by the test train at different speeds
- the stresses in the rail bearers and cross girders produced by service traffic

The loading applied to the bridge by the wheels of the trains was measured using strain gauges on the web of the rails. In order to measure the speed of the trains it was necessary to have at least a second event gauge.

2. STATIC TESTS

2.1 General

For the static tests, at least two cross girders, the adjacent rail bearers and one end cross girder were measured for each bridge. The transducers were situated at the mid span of the elements. Sections with continuity plates were avoided by using immediately adjacent plain sections. The test train approached from each end of the bridge, and stopped at several positions. In order that the results on the different railways might be compared easily, a standard system for numbering the loading-positions and the strain gauges was chosen.

2.2 Conclusions from static tests

- The following two methods of distributing the axle loads between sleepers are recommended and give practically the same good results:

Fig. 2 Distribution of axle loads in length

- The local bending stresses calculated assuming that the rail bearer was continuous and elastically supported on the cross girders, and that the axle load was distributed between adjacent sleepers, produced the best comparison with those measured. However using this assumption means that the overall bridge bending stresses need to be calculated separately.
- Cross girder stresses were calculated assuming that it was part of a frame and the comparison between calculated and measured stresses was reasonable.
- End cross girders have practically built in ends (provided by the bearings of the main girders).

3. DYNAMIC TESTS

3.1 Purpose of the studies

The objects of the dynamic tests with the same test train as used in the static tests are:

- to determine the instantaneous wheel loads during the passage of the train at different speeds, once away and at least once on the bridge.
- to determine the variation in strain produced by the test train at different speeds for a reduced set of measuring points, so that the real dynamic increments, the ratios of the maximum stress which occurs at a given point when a train passes at a certain speed and the maximum static stress caused by the same train, can be deduced as a function of the speed v.

3.2 Dynamic increment $1+\varphi$

UIC leaflet 776-1 R [1] which is relevant to the calculation of railway bridges defines the dynamic factors Φ and $1+\varphi$. The factor Φ is used with the stresses obtained from the design load UIC 71 defined in the UIC leaflet 702-0 [2] ; it takes account of the dynamic effects of different service trains and is a function of the length of the influence line L_Φ and classified according to the state of maintenance of the track.

The coefficient $1+\varphi$ is applied to specific service trains, and its calculation involves not only knowledge of the length L_Φ but also of the speed v of the train and of the natural frequency n_o of the unloaded bridge.

The first task entailed in the theoretical studies of the Committee consisted of checking the formulae for Φ and $1+\varphi$ of UIC leaflet 776-1. These formulae were developed for simply supported beams and their applicability to rail bearers and cross girders were checked.

The dynamic increment φ consists of two components $\varphi' + \varphi''$, φ' depends on the parameter K as follows:

$$K = \frac{v}{2 n_o L_\Phi} \qquad \varphi' = \frac{K}{1-K+K^4}$$

where v = the speed of the train in m/sec
n_o = the natural frequency of the unloaded bridge
L_Φ = the length of the influence line for deflection, given in appendix 2 of the UIC leaflet 776-1.

φ' represents the component of the dynamic effect from perfectly horizontal track, whereas φ'' is the component caused by load variations from unsprung vehicle masses on vertical track irregularities.

The theoretical study of rail bearers and cross girders has proven to be much more complicated than that of the simply supported beam since they are components of a three-dimensional structure, and their dynamic behaviour is greatly influenced by the effect of unsprung vehicle masses. The study is not quite finished and the definitive conclusions will be given in the report ORE D 154 RP 4 which will be edited in 1985.

The following figure 3 shows as an example the maximum values of the measured dynamic increments φ of the PKP bridge against velocity.

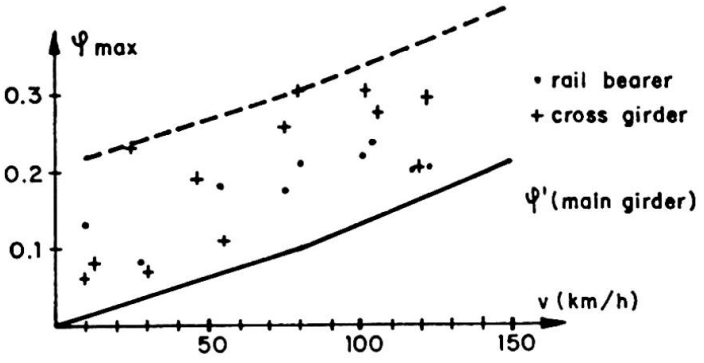

Fig. 3 Measured values of φ_{max} (PKP)

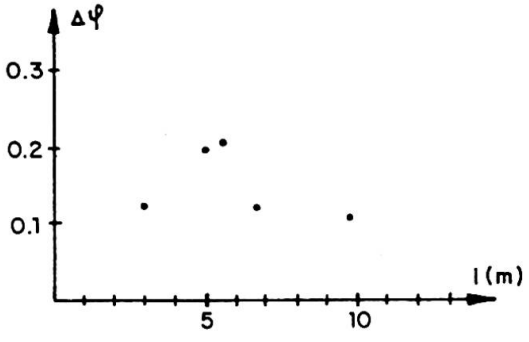

Fig. 4 $\Delta\varphi$ for the 5 bridges

The values for rail bearers and cross girders are drawn separately. Also shown is the curve of φ' for the main girder span L according to the UIC leaflet 776-1 formulae. All values are increasing with velocity and from the results of all five bridges it can be concluded, that φ for both rail bearers and cross girders is approximated by $\varphi' + \Delta\varphi$, where $\Delta\varphi$ may be a function of the cross girder spacing l (Fig. 4).

3.3 Dynamic increment for fatigue $1+\Psi$

The second task is complementary to the first and consists of determining the fatigue damage in the rail bearers and cross girders, expressing it by means of a suitable dynamic increment for fatigue $1+\Psi$, and indicating any relationship with the dynamic increment $1+\varphi$.

$1+\Psi$ will be determined as a function of the speed v and the slope k of the Wöhler line from measured strains due to the test train,

in the following way:

- Step 1

The stress-time history obtained from the passage of the test train at its lowest speed ($v \cong 5$ km/h) is known (Fig. 5).

M for measurement

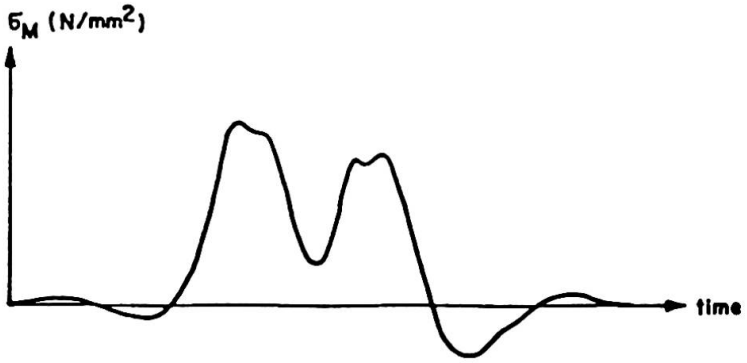

Fig. 5 Measured stress-time history

- Step 2

From this the histogram of stress range $\Delta\sigma_{i,M}$ is obtained using the rainflow counting method and is presented as a multi-stage spectrum. This has to be carried out seperately for every speed of the test train (Fig. 6).

N= number of load cycles

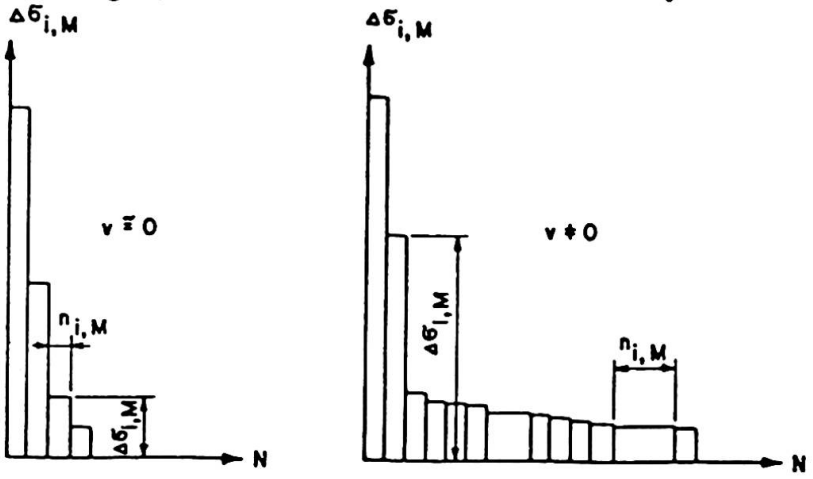

Fig. 6 Multi-stage spectrum

- Step 3

The equal damage single-stage spectrum for every speed v of the test train (v_1, v_2, v_3, ...) are:

$$\Delta\sigma_{e,v,M} = \left[\frac{1}{N_{e,M}} \Sigma n_{i,M} \cdot \Delta\sigma^k_{i,M}\right]^{1/k} \qquad N_{e,M} = \Sigma_i n_{i,M}$$

e for equivalent

- Step 4

By assuming the Palmgren-Miner linear damage summation hypothesis, the single-stage spectra $\Delta\sigma_{e,v,M}$ are transformed into other damage equivalent single-stage spectra $\Delta\sigma_{T,e,v,M}$, with one load cycle per train. We obtain then for the different speeds v different values

$$\Delta\sigma_{T,e,v_1,M}\ ,\ \Delta\sigma_{T,e,v_2,M} \ldots.$$

T for transformed

- Step 5

The dynamic increment for fatigue (Fig. 7) is therefore

$$\Psi = \frac{\Delta\sigma_{T,e,v,M}}{\Delta\sigma_{T,e,v\neq 0,M}}$$

where v= v_1, v_2, ...

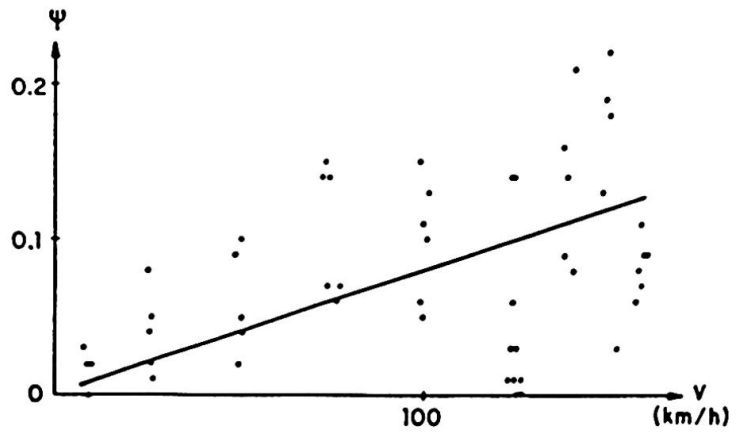

Fig. 7 Dynamic increment for fatigue

A test train (only a locomotive) does not produce many stress ranges, so the first results from the five measured bridges show that the equivalent stress range is about the same as the maximum stress and therefore the dynamic increment $1+\varphi$ is nearly equal to the dynamic increment for fatigue $1+\Psi$.

4. MEASUREMENTS UNDER TRAFFIC

The object of these measurements is to determine the effective loads and resulting stresses in the elements of the bridge during the passage of actual trains in service. The number of trains recorded should be sufficient to permit statistical evaluation of the measured data. About 100 trains, which more or less corresponds to the daily traffic for one track, is considered to be a reasonable number.

It should be pointed out that the purpose of calculating the fatigue damage for an existing bridge differs to some extent from that for a new bridge; the method, however, remains the same.

- For new bridges the fatigue is determined using the loading diagram UIC 71. λ is a load factor by which the stresses taken from the UIC-loading diagram, including dynamic increment Φ, must be multiplied so as to obtain the same accumulated damage as would be caused by the service trains. The simulation of existing loads found in service is effected on the railways using defined, typical, i.e. idealised trains which may over a period of time cause the same type of damage as the trains in service. At the moment, European railways have different and individual typical trains for fatigue considerations.
- In the case of bridges already in use, the load spectrum needs to be determined with the greatest possible accuracy. It is then possible to calculate the damage already caused and also estimate the remaining life, using the same method as for new bridges.

For the purpose of comparison, a single slope Wöhler line, with gradient k= 5, and the linear damage theory of Palmgren-Miner were adopted. The determination of a better, statistically established slope of the Wöhler line, based on different fatigue results which can be found in the literature, is another objective of the Committee ORE D 154. The effect of a double slope Wöhler line will also be considered.

λ-values will be calculated using the different approaches:

$\lambda_{T,typ,M}$ experimental method, using strain measurements for about 100 service trains

$\lambda_{T,typ,C}$ experimental-theoretical method, using measured wheel loads from 100 service trains and the theoretical influence lines.

$\lambda_{T,typ,CC}$ theoretical method, using theoretical influence lines and the axle loads of typical, idealised trains.

By comparing these values λ it is possible to determine the accuracy of the theoretical and experimental-theoretical method by using the pure experimental method. In the ideal case all three values of λ are the same.

In the following, the detailed determination of the values λ is shown for the example of $\lambda_{T,typ,M}$, the others being derived similarly:

- Step 1

  For each service train the stress history σ_M is known from the crossing the bridge (Fig.8).

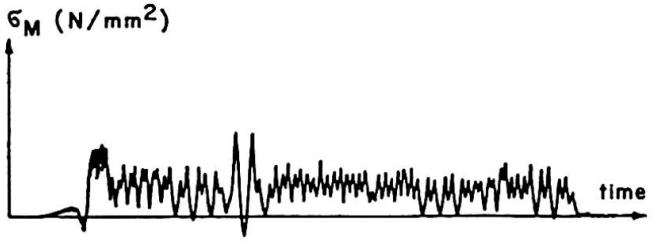

Fig. 8 Measured stress-time history

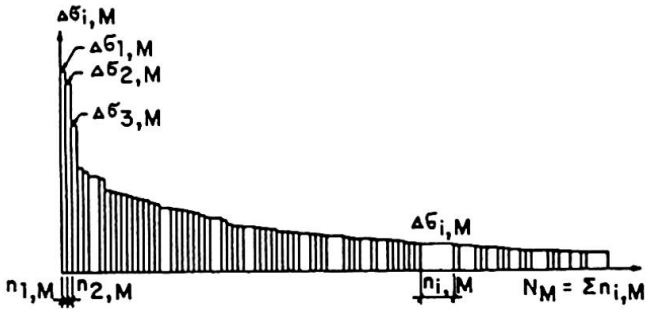

Fig. 9 Multi-stage spectrum

- Step 2

  The histograms of the stress range $\Delta\tilde{\sigma}_{i,M}$ are obtained for each train using the rainflow counting method and presented in the multi-stage spectrum (Fig. 9).

- Step 3

  Determination of the relative stresses $\lambda_{i,M}$ for each service train, using

$$\Delta\sigma_{UIC} = \phi \cdot (\max \sigma_{UIC} - \min \sigma_{UIC}) \text{ and } \phi = \frac{1.44}{\sqrt{L_\phi} - 0.2} + 0.82$$

  we obtain (Fig. 10)

$$\lambda_{i,M} = \frac{\Delta\sigma_{i,M}}{\Delta\sigma_{UIC}}$$

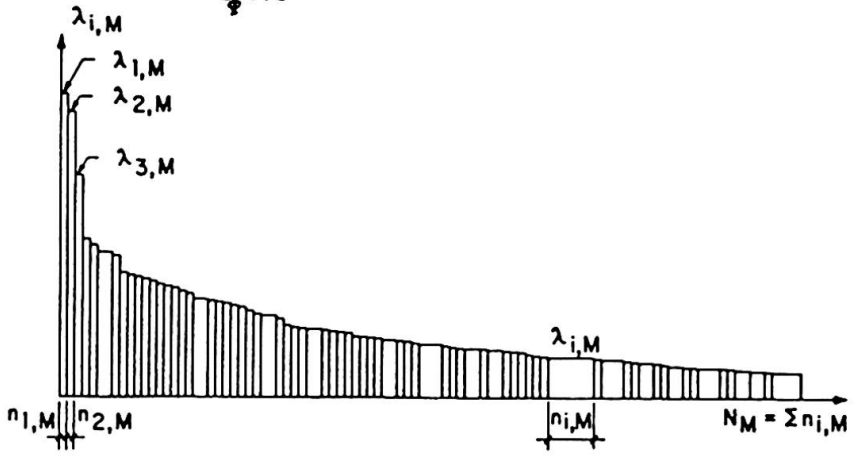

Fig. 10 Related multi-stage spectrum

- Step 4

  Determination of the equal damage single-stage spectrum for each train separately (Fig. 11)

$$\lambda_{e,j,m} = \left[\frac{1}{N_{em}} \Sigma\, n_{i,m} \cdot \lambda_{i,m}^{\,k}\right]^{1/k}$$

  with $N_{em} = \Sigma_i\, n_{i,M}$

  and j as designation of the 100 service trains 1,2,3,.....100

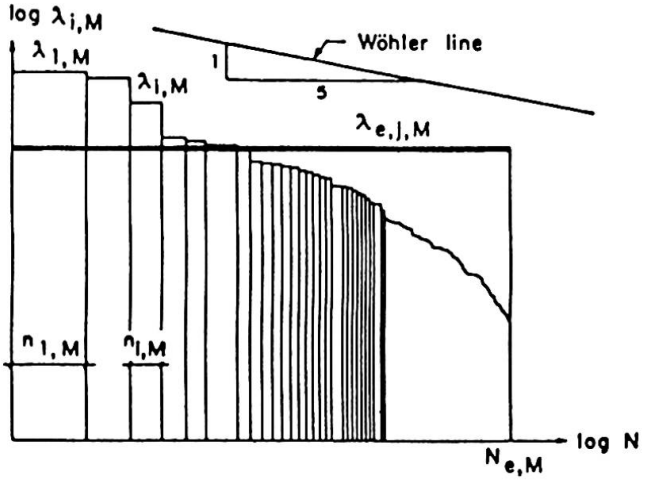

Fig. 11 Single-stage spectrum of instances where damage incurred is equal (heavy line)

- Step 5

Transformation of the single-stage spectrum $\lambda_{e,j,M}$ into another damage-equivalent single-stress spectrum $\lambda_{T,j,M}$ with only one cycle:

$$\lambda_{T,j,M} = \left[\frac{1}{N_T} \cdot \sum_j n_{i,M} \cdot \lambda_{i,M}^k\right]^{1/k} \qquad \text{in which } N_T = 1$$

- Step 6

Combination of all 100 measured transformed single-stage spectra $\lambda_{T,j,M}$

Using: $n_{T,j,M} = 1$ on the assumption that all the 100 service trains differ from each other

$N_{T,B,M} = \sum_j n_{T,j,M} = 100$ service trains (B for service)

$\lambda_{T,j,M}$ see above, transformed single-stage spectrum for one load cycle per service train j

the transformed single-stage spectrum $\lambda_{T,M}$ for the 100 measured service trains is determined as follows:

$$\lambda_{T,M} = \left[\frac{1}{N_{T,B,M}} \sum_{j=1}^{N_{T,B,M}} n_{T,j,M} \cdot \lambda_{T,j,M}^k\right]^{1/k}$$

- Step 7

Determination of $\lambda_{T,typ,M}$ related to the number of the characteristic, i.e. typical service trains specified by a railway ($N_{T,typ,M}$ not equal to the number of measured service trains $N_{T,B,M}$):

$$\lambda_{T,typ,M} = \lambda_{T,M} \left[\frac{N_{T,B,M}}{N_{T,typ,M}}\right]^{1/k}$$

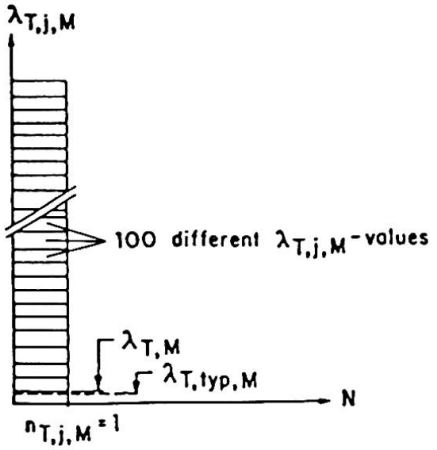

Fig. 12 Composition and transformation of single-stage spectrums

5. REFERENCES

5.1 UIC

Union Internationale des Chemins de Fer, 14 rue J. Rey, F-75015 Paris

[1] UIC leaflet 776-1 R (3rd edition of July 1979)
Loads to be considered in the design of railway bridges

[2] UIC leaflet 702 O (2nd edition of January 1974)
Loading diagram to be taken into consideration for the calculation of rail carrying structures on lines used by international services

5.2 ORE

Office for Research and Experiments, Oudenoord 60, NL-3515 EV Utrecht

[ORE D 154]: Stresses and strength of rail bearers and cross girders of steel railway bridges (presented study)
RP 1 Loading, design and construction, state of technology of different European railways, Sept. 1981
RP 2 Details of strain gauge measurements, Sept. 1981
RP 3 Static studies, Sept. 1984
RP 4 Dynamic studies, to be published in 1985
RP 5 Fatigue studies, to be published in 1985
RP 6 Final report, to be published in 1986

[ORE D 154] is basing on earlier studies [ORE D 128] and [ORE D 130].

New Trends in the Design of Steel Bridges in Czechoslovakia

Tendances nouvelles dans le projet de ponts en acier en Tchécoslovaquie

Neue Tendenzen in der Berechnung von Stahlbrücken in der Tschechoslowakei

J. DJUBEK
Assoc. Prof.
Slovak Academy of Sciences
Bratislava, Czechoslovakia

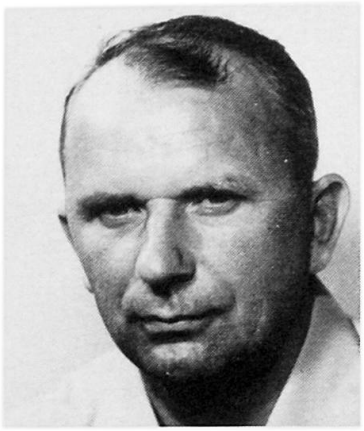

I. KÁRNÍKOVÁ
Dr. Eng.
Czech Technical University
Prague, Czechoslovakia

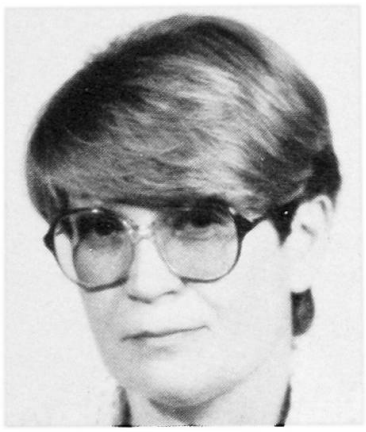

M. ŠKALOUD
Assoc. Prof.
Czech Academy of Sciences
Prague, Czechoslovakia

SUMMARY

The contribution deals with several recent investigations, both theoretical and experimental, into the limit state of plate elements in steel bridges, special attention being paid to the ultimate limit state of longitudinally stiffened compression flanges. On the basis of an analysis of the experimentally determined deformation- and stress states, a definition of the ultimate limit state is presented, and then applied in a theoretical study of the ultimate loads of the longitudinally stiffened compression flanges of steel box girder bridges.

RESUME

La contribution concerne plusieurs études théoriques et expérimentales, de l'état limite ultime des éléments plans des ponts en acier, faisant attention particulièrement à l'état limite ultime des semelles comprimées raidies. Sur la base d'une analyse des états de déformation et de tension déterminés expérimentalement, une définition de l'état limite ultime est présentée, puis appliquée dans une étude de la capacité portante des semelles comprimées raidies des ponts d'acier en caisson.

ZUSAMMENFASSUNG

Der Beitrag behandelt einige neuere theoretische und experimentelle Untersuchungen des Grenzzustandes der Plattenelemente von Stahlbrücken, mit spezieller Aufmerksamkeit auf den Traglastzustand von längs ausgesteiften, gedrückten Gurtplatten. Auf der Grundlage einer Analyse der experimentell festgelegten Deformations- und Spannungszustände wird eine Definition des Traglastzustandes gegeben und dann in einer theoretischen Untersuchung auf die Tragfähigkeit von längs ausgesteiften, gedrückten Gurtplatten stählerner Kastenträgerbrücken angewandt.

1. INTRODUCTION

The necessity to save steel leads in Czechoslovakia to a fast development of thin-walled plated steel structures. In the domain of steel bridgework it is particularly box girder construction that has grown popular with designers. Thus one of the current tasks of the Czechoslovak research is to give enough information about the behaviour of such bridges. As one of the key problems in this line is that of the limit state of longitudinally stiffened compression flanges, the efforts of three departments /i.e. /i/ Department of Bodies Made of Homogeneous Materials at the Institute of Construction and Architecture , Slovak Academy of Sciences, Bratislava, /ii/ the Department of Metal Structures at the Building Research Institute, Czech Technical University, Prague, and /iii/ the Stability Department at the Institute of Theoretical and Applied Mechanics, Czechoslovak Academy of Sciences, Prague, have been combined to contribute to the solution to the above problem. The objective of this paper is to report briefly about the main results of the research.

2. THEORETICAL RESEARCH

One of the Czechoslovak theoretical studies concerning the ultimate limit state of longitudinally stiffened compression flanges was conducted in Bratislava by the first author and his associates.

In this study longitudinally stiffened compression flanges are treated as geometrically orthotropic compressed plates, the solution being corrected in the second stage of the analysis by taking account of the effect of local sheet buckling between longitudinal ribs. The investigation is based on non-linear large deflection theory, the influence of an initial "dishing" /both of the flange as a whole and of its partial sheet panels/ being taken into consideration, and the ultimate limit state is defined /on the basis of the experimental research described below in sec. 3/ by the onset of membrane yielding at the most highly stressed point of the flange sheet.

The ultimate load of the flange is then written as follows:

$$\sigma_{ult} = \sigma_{1N}\, \sigma_{2N}\, R_d\,, \tag{1}$$

where σ_{1N} is the coefficient of global flange buckling, σ_{2N} that of local flange sheet buckling and R_d the s.c. design strength of the flange material /which in the Czechoslovak Limit State Design approach replaces the yield stress R_y; $R_d = 0.87\ R_y$ if $R_y \leq 300$ MPa and $R_d = 0.80\ R_y$ if $R_y > 300$ MPa/.

The large deflection theory analysis is summarized in the following formulae /derived by I. Baláž and the first author/ for the coefficients σ_{1N} and σ_{2N}:

$$\sigma_{lN} = 1 - \frac{\alpha_2}{2}\left[\sqrt{\left(\frac{\psi_1 - \psi_2}{\psi_2}\right)^2 - \frac{2\alpha_3^2}{\sqrt{1+\alpha_2^2}-1}} - \frac{\psi_1 - \psi_2}{\psi_2}\right], \text{ if } \sigma_{lN} \geq 1 - \frac{\alpha_2}{2}$$

or (2a)

$$\sigma_{lN} = 1 - \alpha_2 \frac{2\alpha_3^2 - \frac{\psi_1 - \psi_2}{\psi_2}\left(\sqrt{1+\alpha_2^2}-1\right)}{2\alpha_3^2 + \sqrt{1+\alpha_2^2}-1}, \text{ if } \sigma_{lN} \leq 1 - \frac{\alpha_2}{2} \quad (2b)$$

where

$$\alpha_2 = 0.835 - 0.04\alpha + 0.01\,\frac{\lambda}{100} \quad (3)$$

α being the side ratio of the flange panel ($\alpha = a/b$) and λ its width-to-thickness ratio ($\lambda = b/t$),

$$\alpha_3 = 0.14\alpha + 0.127, \quad (4)$$

$$\psi_1 = \frac{B_x}{B} - \frac{12\nu^2}{1-\nu^2\frac{D}{D_x}}\left(\frac{e_{st}}{t}\right)^2 - 2\alpha^2\left(1 + \frac{GJ_{t,st}}{2Bb_{st}}\right) + \alpha^4,$$

B denoting the flexural rigidity of the flange sheet ($B = Et^3/12(1-\nu^2)$), B_x that of the longitudinally stiffened flange ($B_x = B + Ete_{st}^2/(1-\nu^2) + EJ_{st}/b_{st}$), D the normal rigidity of the flange sheet ($D = Et/(1-\nu^2)$), D_x that of the longitudinally stiffened flange ($D_x = D + EA_{st}/b_{st}$), e_{st} the distance of the centroid of a cross-section having its area equal to $A_{st} + b_{st}t$ (where A_{st} is the area of one longitudinal stiffener, t the thickness of the flange sheet and b_{st} the spacing of the longitudinal ribs),

ν Poisson's ratio of the flange material, G its elasticity modulus in shear. I_{st} the moment of inertia of one longitudinal stiffener with respect to the centroidal axis of the cross-section $A_{st} + b_{st}t$ and $I_{t,st}$ the moment of inertia in tension of one longitudinal rib

$$\psi_2 = (\delta_x - \nu^2)\,\frac{\alpha^2\lambda^2}{720}\,\frac{R_d}{210}, \quad (5)$$

δ_x designating the ratio D_x/D.

The local sheet buckling coefficient is worked out as follows:

$$\varphi_{2N} = \frac{\varphi_N + A_{st}/(b_{st}.t)}{1 + A_{st}/(b_{st}.t)} \tag{6}$$

where for boundary flange sheet panels

$$\varphi_N = \frac{40}{\frac{b_{st}}{t} + 10} \sqrt{\frac{210}{R_d}} \tag{7a}$$

and for inner sheet panels

$$\varphi_N = \frac{40 \sqrt{\frac{210}{R_d}}}{\frac{b_{st}}{t} + 10} \left(1.3 - \frac{12 \sqrt{\frac{210}{R_d}}}{\frac{b_{st}}{t} + 10}\right), \tag{7b}$$

the design strength, R_d, of the flange material being inserted in MPa. The above two formulae were derived by Z. Sadovský and the first author.

The aforesaid orthotropic plate approach is currently being complemented in Bratislava by an analysis of the ultimate limit state of flanges fitted with discrete stiffeners, which case is of practical importance when the number of longitudinal ribs is so small that the orthotropic plate approach is not acceptable. The theoretical studies conducted in Prague at the moment are centred on /i/ a non-linear large deflection variant of folded plate theory and /ii/ the problem of the interaction that exists in wide flanges between shear lag and flange buckling, this latter investigation being performed in cooperation with University of Liège.

3. EXPERIMENTAL RESEARCH

One of the experimental studies that have recently been carried out by the second and third authors in Prague also deals with the limit state of longitudinally stiffened compression flanges.

Two series of box girders were tested. The objective of the first series of experiments, comprising four girders, was to look into the difference in behaviour between /a/ compression flanges fitted with /a_1/ single-sided and /a_2/ double-sided longitudinal ribs and /b/ compression flanges stiffened by /i/ a small number of bulky ribs and /ii/ a large number of flexible ribs. In the other series of experiments, conducted on eight test girders /see Fig. 1/, the number of longitudinal stiffeners was kept constant, but their size and the aspect ratio of the flange panel varied.

The buckled pattern of the compression flange was carefully measured by means of the stereophotogrammetric method. Thanks to a great number of strain gauges being attached to both sides of the flange sheet and of the longitudinal stiffeners, the stress state, the progression of plasticization and the formation of a failure mechanism in the flange was studied.

It has been concluded that the ultimate limit state of longitudinally stiffened flanges of steel box girder bridges can be determined either by the onset of membrane yielding in the flange sheet or by the onset of plasticization in the stiffeners. In the context of the modified orthotropic plate approach /sec. 2 hereabove/, only the onset of membrane yield in the flange sheet can be reflected. Then two question arise:

1. Does the ultimate load calculated via the above definition of the ultimate limit state provide enough safety, or - on the other side - is it not too conservative, with respect to the actual experimental load carrying capacity?

2. Is not the safety of a compression flange, designed via the above approach, jeopardized in the case of steel bridges, subject to intensive variable repeated and dynamic loadings, by local plasticization which occurs in the flange, for example, due to the effects of the peaks of bending stresses that arise as a result of "breathing" of the flange sheet and are not checked by the above definition of the ultimate limit state?

TEST GIRDER		LONGITUDINAL STIFFENER	P_{ult} / kN /	YIELD STRESS /MPa FLANGE	STIFFENER
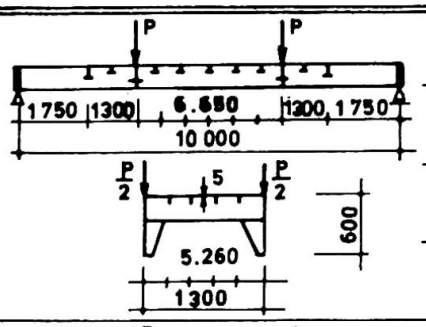	TG 1	-	450	461	-
	TG 2	35.8	680	429	374
	TG 3	55.8	828	391	311
	TG 4	65.8	920	391	414
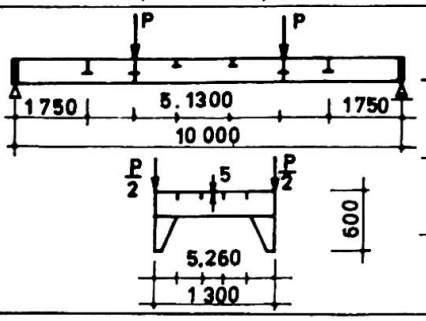	TG 5	-	450	490	-
	TG 6	55.12	800	242	?
	TG 7	90.12	1060	431	287
	TG 8	110.12	1100	439	432

As for the first question, the experimental results show that - in the case of the authors' test girders - the plastic reserve of the onset-of-membrane yielding loads with respect to the failure loads was of about 25%; i.e. it can be regarded as fitting for the compression flanges of steel box girder bridges.

In order to give a reply to the other question, the second and third authors analysed in detail the membrane and bending stresses that occurred in the compression flanges of the test girders at different levels of the load and came to the conclusion that their intensity was such that at loadings lower than the above defined ultimate loads /and the more so at loadings which would correspond to the level of the working loads of the structure/no danger of incremental collapse or low-cycle fatigue developed.

As the large-scale girders /of length $l = 10$ m and fabricated following exactly the technique used in the production of ordinary steel bridges/ tested in Prague can be regarded as reasonably representative for steel box girder bridges, it can be anticipated that the aforesaid conclusions hold generally.

Thus, it is concluded that the onset of membrane yielding can serve as a reliable definition of the ultimate limit state of the longitudinally stiffened compression flanges of steel box girder bridges, and may safely be employed in theoretical analyses such as that presented hereabove in sec. 2.

Another extensive experimental investigation conducted currently by the second and third authors in Prague deals with the ultimate limit state of longitudinally stiffened webs subjected to partial edge loading. This problem is of importance , for example, when a bridge structure is "launched out" into its definitive position above the river. 94 girders have been tested to date. It has been concluded that the effect of the longitudinal stiffener on an increase in ultimate load is significant /in the authors´tests it amounted to 30-45%/ only when the stiffener is located close ($b_1 \leq b/4$, b being the web depth) to the loaded flange and its size is sufficient for the stiffener to behave as a fully effective one. Formulae for the optimum rigidity of such a stiffener and for the ultimate loads of such webs were also derived.

4. COMPARISON BETWEEN THEORY AND EXPERIMENTS

It is of interest to check how the theoretical approach presented in sec. 2 correlates with the results of the experiments on longitudinally stiffened flanges described in sec. 3. An analysis of the experimental conclusions shows that the predicted ultimate loads correlate very well /the difference amounting merely to less than 10% on the safe side/ with the experimental onset-of--membrane yielding loads - as it should be. For this reason this approach has been incorporated /as one of the two normative approaches for the design of stiffened compression flanges, the other one being based on a bar simulation analogy/ into the new edition of the Czechoslovak Design Code for Steel Bridges.

Alternating Plasticity Analysis of an Industrial Frame

Analyse plastique d'un cadre dans la construction lourde

Traglastanalyse eines Stahlrahmens im Industriebau

Ante VUKOV
Professor
Civil Engineering Institute
Zagreb, Yugoslavia

Ante Vukov, born 1936, received his Civil Engineering Degree from Zagreb University and his Doctorate from the Catholic University of America, Washington, D.C. After spending over 15 years in industry and consulting work Dr. Vukov is currently on the academic staff of the Civil Engineering Institute.

SUMMARY

The basic postulates of the limit analysis of structures are valid when the applied loads are acting simultaneously and are increased proportionally in their magnitude without reversing the direction until limit load is reached. If this is not the case, the carrying resistance of the structure may be reduced to shake-down load due to influence of the variable repeated loading. An industrial steel frame has been analyzed under variation of the specification snow and wind loads as given in specifications and the obtained results are discussed.

RESUME

Les postulats de base de l'analyse limite sont valables lorsque les charges appliquées le sont simultanément et croissent constamment jusq'à la rupture. Si ce n'est pas le cas, la résistance de la structure peut être réduite à la charge "Shake-down", à cause de l'influence d'une charge répétée variable sur la structure. Le cadre d'une structure industrielle a été analysé sous l'effet de charges variables de neige et de vent – définies dans les normes – et les résultats sont discutés.

ZUSAMMENFASSUNG

Die Grundanforderungen der Grenzanalyse gelten für die Belastungen, die ohne Richtungsänderung gleichzeitig wirken und stetig bis zur Grenzlast wachsen. Andernfalls kann die Tragfähigkeit der Konstruktion durch sogenannte "shake-down"-Lasten, d.h. durch wechselnde Lastwirkungen, vermindert werden. Im gegebenen Fall wurde ein Industrie-Stahlrahmen aufgrund der wechselnden Norm-Belastungen aus Schnee und Wind untersucht, die Ergebnisse verglichen und erläutert.

1. INTRODUCTION

The actual loads may vary considerably and change indenpendently of each other during the lifetime of a structure. Such loads as termed as variable repeated loads. Under such load variation, as first recognized by M.Grüning (1926) and G.Kazinczy (1931), the structure may fail under considerably lower loads than computed applying the limit analysis basic postulates. W.Prager (1948) first used the term shakedown loads, as the largest set of loads under which a structure is safe against failure under variable repeated loads.

As in the case of the limit load, the concept shake down load has a precise mathematical meaning only for idealized materials. The contributions of strain hardening are ignored. The Bauschinger effect is also disregarded.

Two types of the problem may be encountered when variable repeated loading is acting on a structure and they are differentiated as:

(a) alternating plasticity collapse, at load factor $\lambda_s = \lambda_a$, and

(b) incremental collapse, at load factor $\lambda_s = \lambda_i$.

In the alternating plasticity problem, failure occurs at a relatively small number of load cycles when the repeated loading is such that yielding of the material at the structure critical sections occurs alternately in tension and compression. When plastic flow occurs in reverse direction, material at the given section accumulates a certain amount of plastic work encircled by the M_p/Θ curve (Fig. 1). The structure can tolerate only a limited amount of plastic work. After this limit is reached, the material is weakened or becomes more brittle. This effect is similar to high-cycle elastic fatique, but the number of cycles of load application involved is only of order of tens or hundreds. During each cycle of loading the plastic flow will increase and eventually lead to structure member fracture at the load factor λ_a.

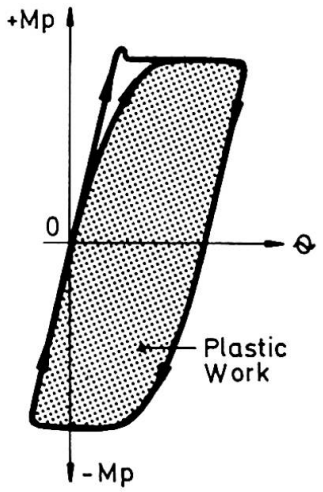

Fig. 1 Plastic work limit

In the cases just described, when the history of loading corresponds to plastic reversals in some parts of the structure, it is neccesary to evaluate the condition of reliability of alternating plasticity low cycle fatique collapse. Reduction of the structure carrying capacity should be expressed by the magnitude and number of plastic reversals. A critical number of reversals can be accumulated in a relatively short time depending on the nature of loading.

According to present specifications the plastic theory is applied to the design of structures under predominantly static loads. In these specifications there are no specific requirements related to the shake-down problem.

2. FUNDAMENTALS

Failure of a structure due to alternating plasticity will not occur when there exist such ranges of bending moment values for which a section behaves elastically. This condition may be stated as:

$$(M_i^e)_{max} - (M_i^e)_{min} \leq 2M_p/\alpha \qquad (1)$$

Where,

$(M_i^e)_{max}$ = Maximum elastic bending moment at section i,

$(M_i^e)_{min}$ = Minimum elastic bending moment at section i,

M_p = Full plastic moment at section i,

α = Cross section shape factor.

In the incremental collapse problem an increase in deflection occurs during each cycle of loading. It is necessary to find a load factor λ_i for which increments of deflection stop after several load cycles and overall deflection ceases to increase. Failure of a structure due to incremental collapse will not occur when the sum of residual moment and elastic moment of applied loading on the structure do not exceed the full plastic moment value at any given section, i.e.

$$(M_i^e)_{max} + m_i^r \leq M_p \qquad (2)$$

Where,

$(m_i^e)_{max}$ = Maximum elastic bending moment at section i assuming that yielding does not occur,

m_i^r = Residual bending moment at section i,

M_p = Full plastic moment at section i.

The loads that exceed the incremental shakedown load are found to gradually cause structure failure due to excessive deflections. The above conditions for shakedown load should be checked at every section i where:

- concentrated load is applied,
- at the joint of two or more structure elements, and
- where element changes section properties.

For the ordinary low frame structure the structure failure is more likely to occur due to alternating plasticity than to incremental collapse [9] . In the application of the plastic method to the design of the structure, strength is the major criterion. It is necessary, however, also to check other safety criteria such as local stability, overall stability, deflections, and if main load is variably repeated, the shakedown collapse. The most up to date research of structures under variable repeated loads has been performed on ideal structures. A 12 m industrial frame is analyzed under variable repeated loads given by load specification [11] , as follows:

- snow load: S = from 0.00 to +0.75 kN/m², and
- wind load: W = from -1.10 to +1.10 kN/m².

The whole structure is made of IPE 240 from mild steel (A36) with yield stress of 236 N/mm².

3. AN INDUSTRIAL FRAME ANALYSIS

Fig. 2 shows an outline of the frame, its section properties, gravity and wind loading on the frame.

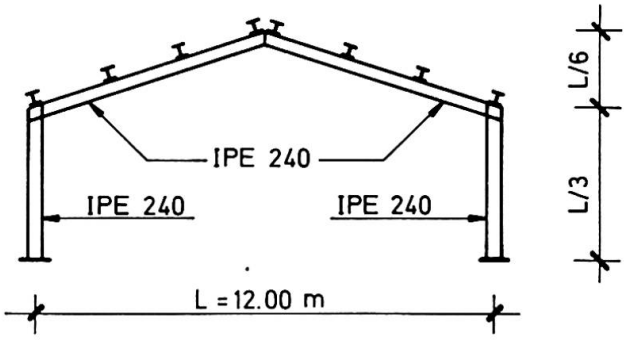

a) Structure

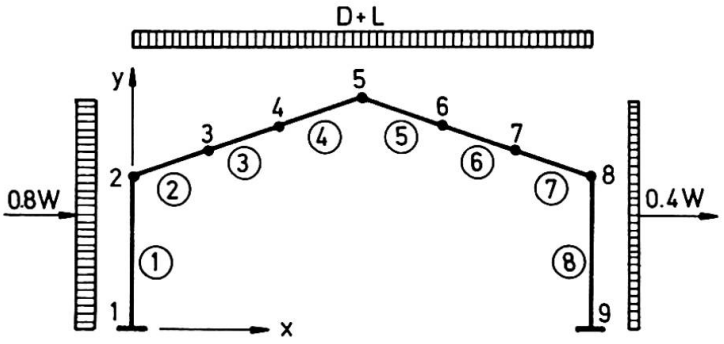

b) Loading

Structure Properties:

IPE 240
$A = 39.1\ cm^2$
$I_x = 3\,890\ cm^4$
$M_p = 8\,638\ kN\,cm$

Gravity Loads:

$D = 0.417\ kN/m^2$
$L = 0.750\ kN/m^2$
$D+L = 1.167\ kN/m^2$

Wind Load:

$W = 1.10\ kN/m^2$

Load Combinations [kN]

Joint	DL+LL		DL+LL+W	
	P_x	P_y	P_x	P_y
2	0	-7.0	11.44	-9.5
3	0	-14.0	1.68	-19.0
4	0	-14.0	1.68	-19.0
5	0	-14.0	1.68	-14.0
6	0	-14.0	1.68	-9.0
7	0	-14.0	1.68	-9.0
8	0	-7.0	6.12	-4.5

Fig. 2 Frame properties and loadings

3.1 Limit load calculation

(a) Case I - Dead load + Live load

From the principle of virtual displacements, the interior and exterior work on the structure collapse mechanism may be equated, i.e.

$$6M_p\theta = 9P_uL\theta/6 \quad \text{or}$$
$$P_u = 4M_p/L = 4 \cdot 8638/1200$$
$$P_u = 28.793\ kN.$$

$P_u = 28.793$ kN
$\lambda_c = 2.057$
$\Delta_c = 15.66$ cm

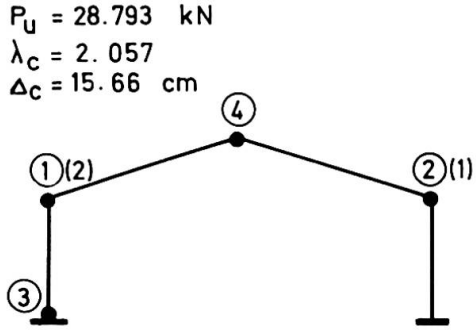

(a) Formation of hinges

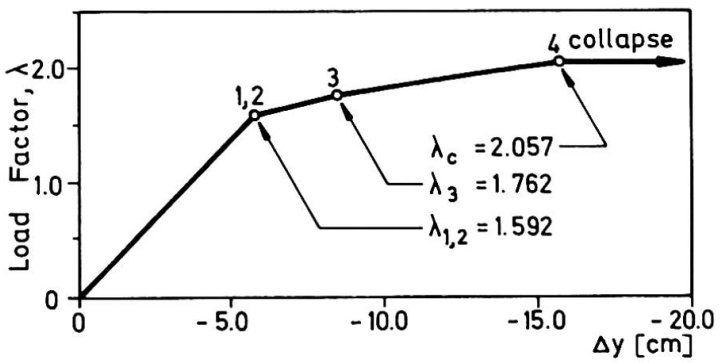

(b) Vertical deflection at joint 5

Fig. 3 Formation of plastic hinges and vertical deflection at joint 5

Collapse load factor:

$$\lambda_c = P_u/P = 28.793/14.0$$
$$\lambda_c = 2.057 > \lambda_{req} = 1.70 \text{ (see Refs. 1,4,6,12)}$$

Maximum vertical deflection of the frame occurs at the ridge line (joint 5). Deflection of joint 5 and hinge formation history is shown in Fig. 3. First and second plastic hinge are to be formed at eave lines at load P=22.37 kN. The last hinge is to be formed at ridge line at load P=28.79 kN and vertical deflection of -15.66 cm. For this case of loading the structure is overdesigned 21% (=0.357/1.7).

(b) Case II - Dead load + Live load + Wind

Similarly, as it was done in Case I, equating the internal and external work on the collapse mechanism, the collapse load is obtained:

$$P_u = 23.466 \text{ kN}, \quad \text{at the collapse load factor}$$
$$\lambda_c = 1.676 > \lambda_{req} = 1.50 \text{ (see Refs. 4,13),}$$
$$= 1.36 \text{ (see Ref. 6), and}$$
$$= 1.30 \text{ (see Ref. 1).}$$

The structure has an additional carrying capacity of 11.7% (=0.176/1.50). The maximum deflection occurs at lee-ward wind eave (joint 8). The plastic hinge history formation and deflection of joint 8 are shown in Fig. 4.

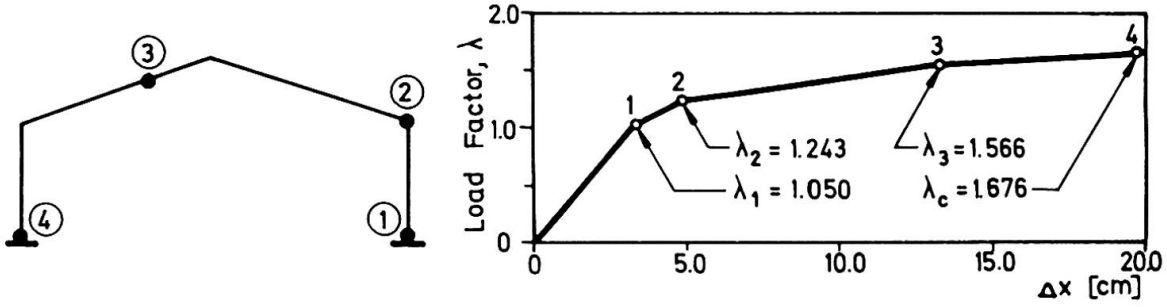

(a) Formation of hinges (b) Horizontal deflection at joint 8

Fig. 4 Formation of plastic hinges and horizontal deflection at joint 8

3.2 Alternating plasticity collapse analysis

For the given specification loads the elastic bending moments at critical sections obtained by the second-order analysis are shown in Table 1.(in kNcm).

	Loading		Section								
	Hor.	Vert.	1	2	3	4	5	6	7	8	9
1	O	D	1615	-1935	- 20	895	805	895	- 20	-1935	1615
2	O	L	2910	-3495	- 40	1615	1460	1615	- 40	-3495	2910
3	O	D+L	4540	-5460	- 65	2530	2290	2530	- 65	-5460	4540
4	W	O	-4050	1495	2050	1490	-180	-1615	-1935	-1135	3700
5	-W	O	3700	-1135	-1935	-1615	-180	1490	2050	1495	-4050

Table 1. Elastic bending moments for specified loading

Using the value for elastic bending moments from Table 1 , the shakedown factors for alternating plasticity are calculated using Eq. (1). The loading cycles a, b, and c are combined as follows:

Cycle a - load combination (2),(4) and (5)

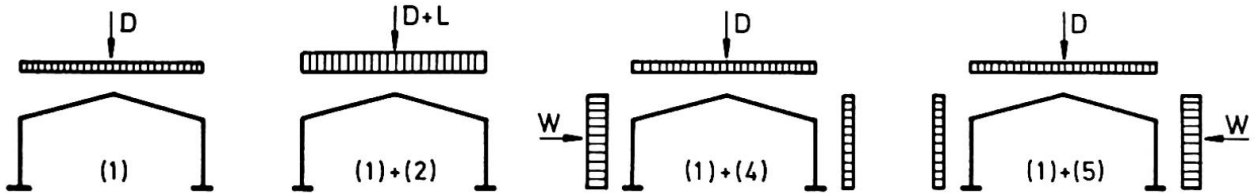

M_i^+	6610	1495	2050	3105	1460	3105	2050	1495	6610
M_i^-	-4050	-4630	-1975	-1615	- 360	-1615	-1975	-4630	-4050
$M_i^+ - M_i^-$	10660	6125	4025	4720	1820	4720	4025	6125	10660

Table 2 Cycle a - Extreme bending moments for load combination (2), (4) and (5)

Applying Eq. (1) and using moment value from Table 2 the load factor is:

$$\lambda_{s,a} = \frac{2M_p}{(M_i^e)_{max} - (M_i^e)_{min}} \cdot \frac{1}{\alpha} = \frac{2 \cdot 8638}{10660} \cdot \frac{1}{1.13}$$

$\lambda_{s,a}$ = 1.434 (Resistance of the structure is reduced to 1.434/1.676 = 0.856)

Cycle b - load combination (3),(4) and (5)

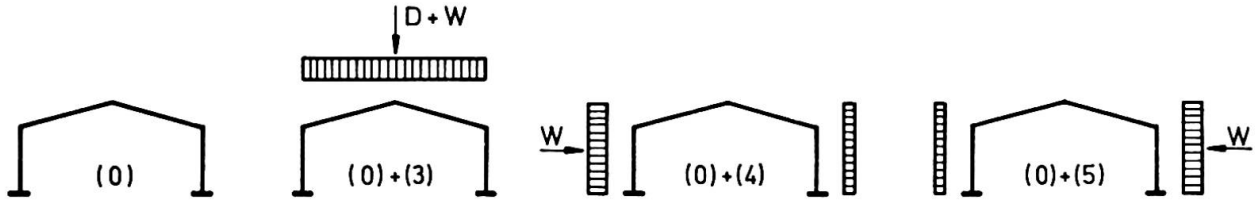

M_i^+	8240	1495	2050	4020	2290	4020	2050	1495	8240
M_i^-	-4050	-6595	-2000	-1615	- 360	-1615	-2000	-6595	-4050
$M_i^+ - M_i^-$	12290	8090	4050	5635	2650	5635	4050	8090	12290

Table 3 Cycle b - Extreme bending moments for load combination (3),(4) and (5)

The load factor for cycle b:

$$\lambda_{s,b} = \frac{2 \cdot 8638}{12290} \cdot \frac{1}{1.13}$$

$\lambda_{s,b}$ = 1.244 (Resistance of the structure is reduced to 1.244/1.676 = 0.742).

Cycle c - load combination (3),(-3) and (5)

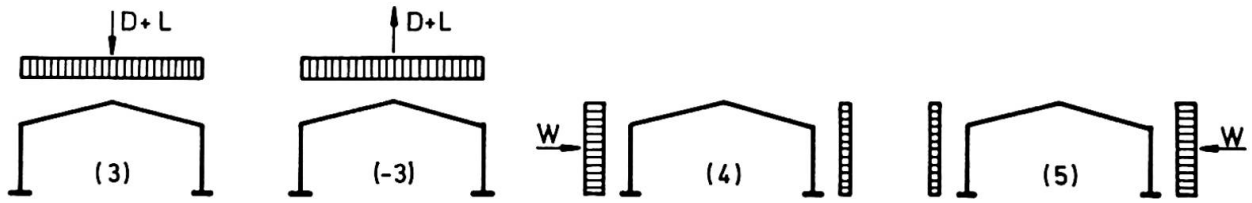

M_i^+	8240	6955	2115	4020	2290	4020	2115	6955	8240
M_i^-	-8590	-6595	-2000	-4145	-2650	-4145	-2000	-6595	-8590
$M_i^+ - M_i^-$	16830	13550	4115	8165	4940	8165	4115	3550	16830

Table 4 Cycle c - Extreme bending moments for load combination (3),(-3),(4) and (5)

The load factor for cycle c:

$$\lambda_{s,c} = \frac{2 \cdot 8638}{16830} \cdot \frac{1}{1.13}$$

$$\lambda_{s,c} = 0.908$$

A coefficient of the load variation k_s equals to a ratio of alternating plus 50 per cent of loading to the overall load acting on the structure. For the considered loading cycles the following values are obtained:

$$k_{s,a} = (25.96+0.5 \cdot 54.0)/109.96 = 0.482$$
$$k_{s,b} = (26.96+0.5 \cdot 84.0)/109.96 = 0.618, \text{ and}$$
$$k_{s,c} = 109.96/109.96 = 1.000$$

The load cycle c corresponds to alternating of the total load acting on the structure in practical sense, but not in a true mathematical meaning because of the wind suction effect at the leeward side of the building.

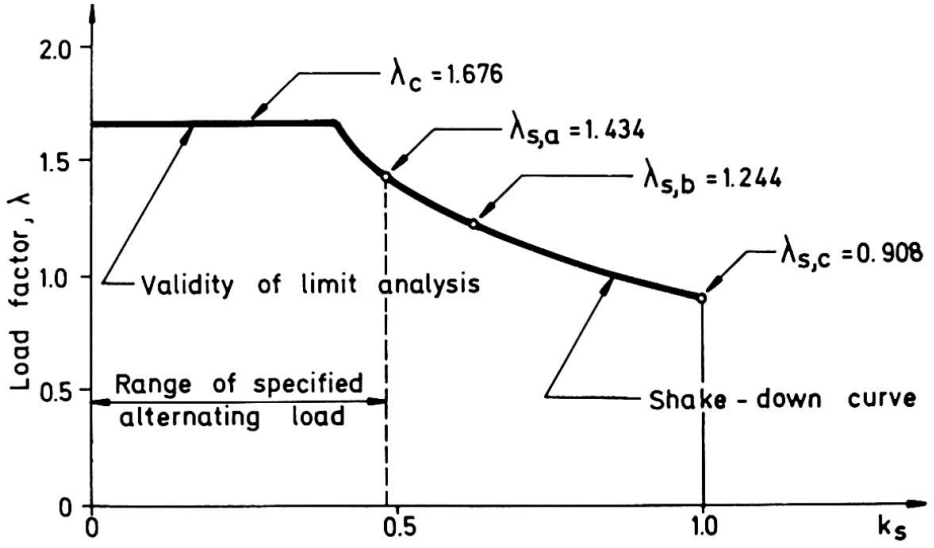

Fig. 5 Range of limit analysis and shake-down validity

In Fig. 5 the limit analysis validity range is represented by a horizontal line at $\lambda_c = 1.676$. The curved line shows the reduction of the structure resistance due to variation of repeated loads.

4. CONCLUSIONS

The effect of specification repeated loads on an industrial steel frame was investigated and the following conclusions can be drawn:

- The reduction of the structure carrying resistance under specification variable loading was 14.4 per cent (load cycle a);
- If the total vertical load was variably repeated then the carrying resistance reduction of the structure would be 25.8 per cent (load cycle b);
- Up to the load ratio k=0.40 there is no theoretical reduction of the structure carrying resistance due to variable repeated loading given in the specification.

Some countries are practising plastic design of steel structures [1,2,4,6,8], and others are presently in the process of either adapting or considering adaptation of their editions of steel design specification based on limit analysis and plastic design. The reduction of the carrying resistance in the considered example seems extensive and cannot be compensated by strain hardening. In view of this the limit of "predominantly static load" in these specifications should be more precisely defined for which the analysis due to variation of repeated loads is not required.

REFERENCES

1. AISC Manual of Steel Construction, American Institute of Steel Construction, Inc., New York, 1969.
2. ASCE, Plastic Design in Steel, American Society of Civil Engineers, New York, 1971.
3. BEEDLE, L.S., Plastic Design of Steel Frames, John Wiley & Sons, Inc., New York, 1958.
4. DIN 1050 - Traglastverfahren, DAST Richtlinie 008, März 1973.
5. HODGE, F.G., Plastic Analysis of Structures, McGraw-Hill Book Co., New York, 1959.
6. MORRIS, L.J., and RANDALL, A.L., Plastic Design, Constructional Steel Research Development Organization, Croydon, Great Britain, 1975.
7. NEAL, B.G., The Plastic Methods of Structural Analysis, A Halsted Press Book, New York, 1977.
8. NORM SIA 161/1979, Schweizerische Zentralstelle für Stahlbau, 8034 Zürich.
9. PERRONE, N., Limit Analysis of Structures (lectures), Catholic University of America, Washington, D.C., 1976.
10. PRAGER, W., Problem Types in Theory of Perfectly Plastic Materials, Journal Aeronaut, Sci., 15, 1948.
11. SLUŽBENI LIST SFRJ, Tehnički propisi za nosive čelične konstrukcije, (Technical Standard for Steel Structures), Belgrade, br. 41/1964.
12. VUKOV, A., A Review of some Problems in Plastic Design, (in Croatian) Proceedings of First Yugoslav Symposium on Theory of Plasticity, Plitvice, Yugoslavia, 1981., pp. 70-77.
13. VUKOV, A. and PEROŠ, B., Plastic Analysis and Design of Steel Structures, (in Croatian) Symposium "Steel Structures to-day", Special Publication, Belgrade, February 24-25, 1983, pp. 329-351.

Statistical Study of Resistance of Steel Members

Etude statistique de la résistance d'éléments de construction métallique

Statistische Untersuchung der Tragfähigkeit von Bauteilen aus Stahl

Tetsuro ONO
Dr. Associate Prof.
Nagoya Inst. of Tech.
Nagoya, Japan

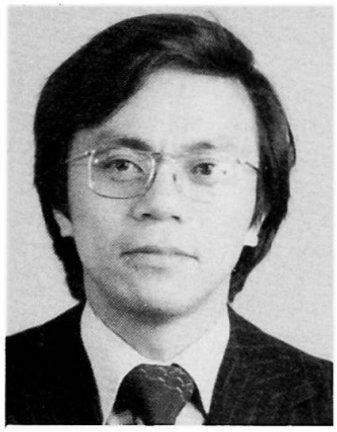

T. Ono, born 1944, graduated from Nagoya Inst. of Tech. in 1968. Took Dr. degree at Tokyo Inst. of Tech. in 1976. He is Associate Prof. at Nagoya Inst. of Tech., department of architecture since 1979. His special research interests are stability problems, aseismic design and system reliability.

Tomiyuki HIRANO
Struct. Engineer
Nikken Sekkei Ltd.
Osaka, Japan

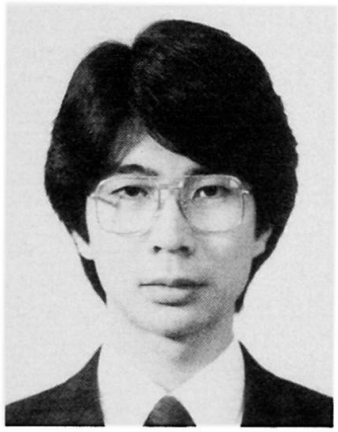

T. Hirano, born 1958, graduated from Nagoya Inst. of Tech. in 1981. He took his M.Sc. degree at Nagoya Inst. of Tech. in 1983. He is at present structural engineer of Nikken Sekkei Ltd.

SUMMARY

This study presents a reliability-based design method for structural steel frames, which enables the designer to control numerically the structural safety. It allows to compute and formulize the statistical resistance values of members, on the basis of widely varying experimental data.

RESUME

L'étude présente une méthode de calcul de charpentes métalliques, fondée sur la notion de fiabilité et permettant au projeteur de contrôler numériquement la sécurité structurale. La méthode permet aussi – sur la base de valeurs expérimentales – de calculer une valeur statistique de la résistance des éléments de la charpente.

ZUSAMMENFASSUNG

Der Beitrag beschreibt ein Bemessungsverfahren für Rahmentragwerke aus Stahl, das sich auf die statistische Erfassung der Materialfestigkeit abstützt. Es erlaubt dem projektierenden Ingenieur die Bruchsicherheit numerisch zu kontrollieren und den Widerstand des Tragwerkes aufgrund experimenteller Daten statistisch zu erfassen.

1. INTRODUCTION

Building structures can never be free from initial imperfections, nonuniformity of material properties, variation of constraint on structural connections, irregularities of loads and uncertainties in analysis of load transfer when the loads are converted to load effects. Hence, the safety of structures cannot be discussed without considering these uncertain factors. When remarkable progress in precision of fabrication of members and in techniques of structural analysis are considered, it is highly desirable that a reliability-based design method predicated on a probalistic approach be put in practical use. However, it still appears that some more time will have to be elapsed before such method can be commonly accepted in design practice. In this connection, the insufficiency of statistical information on these uncertain factors may be pointed out as a major factor which is preventing the early acceptance of such methods.

This research is intended to estimate the limit performance to the maximum extent, to present a design method which can control the scale of structural safety by numerical values, to substantiate the statistical information on the member resistance which is pointed out to be particularly insufficient, and to define clearly in the framework of statistics the real meaning of design strength as set out in various design criteria currently in use.

2. INTRODUCING FAILURE CRITERIA

The design method by the use of standardized values is developed beginning with the derivation of the failure probability of structures. In development of the following formulas, upper case letters are used to indicate random variables and the standard random variable, mean value and standardized deviation of X are expressed by $\tilde{X}$, $\bar{X}$ and σ_x respectively. In Fig. 1, the resistance and the load effect are expressed as independent normal random variables R and S respectively and the failure region $R < S$ is expressed by the standardized coordinate $\tilde{R} - \tilde{S}$. Then, the joint probability density function $f(\tilde{R}, \tilde{S})$ in this coordinate is expressed by the following formula:

$$f(\tilde{R},\tilde{S}) = \phi(K) \,/\, \sqrt{2\pi} \tag{1}$$

in which $\phi(\ )$ is the standard normal probability density function, and K is equal to $\sqrt{\bar{R}^2 + \bar{S}^2}$. Since the failure standardized value k_f is given by shortest distance from the origin to the boundary, k_f and the failure probability p_f may be expressed as follows:

$$k_f = (\bar{R} - \bar{S}) \,/\, \sqrt{\sigma_R{}^2 + \sigma_S{}^2} \tag{2}$$

$$p_f = \iint_{\sigma_R \cdot \tilde{R} - \sigma_S \cdot \tilde{S} + \bar{R} - \bar{S} < 0} f(\tilde{R}, \tilde{S}) d\tilde{R} d\tilde{S} \qquad = 1 - \Phi(k_f) \tag{3}$$

where $\Phi(\ )$ is the standard normal distribution function.
In applying to the design the failure probability thus derived, it is general practice to establish the allowable failure probability p_d firstly and then proceed with the design within the allowable range of p_d. Thus,

$$p_f = 1 - \Phi(k_f) < p_d \tag{4}$$

However, p_f which is necessary for the design presents itself as a problem generally at the skirt of the probability distribution, and it shows a delicate reaction even to minute changes in k_f. To provide a practical solution to such problem, the above formula is transformed as follows:

$$\Phi^{-1}(1 - p_d) < k_f \tag{5}$$

In the above formula, the term $(1 - p_d)$ is a probability indicating the reliability which is a complementary event of failure, and thus $\Phi^{-1}(1 - p_d)$ indicates

the standardized value in the standard normal distribution. If this is defined as a design standardized value, then k_d and k_f can be checked on the same order. In this case, k_d is determined on the basis of engineering judgement by adjusting it to the requirements of the existing design criteria and by considering the significance of the structure. Any probability distribution other than the normal distribution may be considered by two methods. In one method, a corrective coefficient is obtained for each distribution pattern and k_f is multiplied by such coefficient. In this case, even the value of p_f can be obtained at the time of designing. For computation of the corrective coefficient, the failure probability is obtained first by the Monte Carlo simulation, and then the analytical value is converted to the standardized value in the standard normal probability distribution. As an alternative, the standardized value converted in the same manner as described above may be compared with k_f, and k_d itself may be corrected for each distribution. In this report, the first manner described above is followed, but k_f is presented without being modified to reflect the distribution. Consequently, from this k_d, the design of members having a reliability of $\Phi(k_d)\%$ is carried out to satisfy the following formula:

$$k_f = (\bar{R} - \bar{S}) \,/\, \sqrt{\sigma_R{}^2 + \sigma_S{}^2} > k_d \tag{6}$$

Where the unity of various loads is involved, each load effect S_j is regarded as acting independently, and the load effect is obtained by the following formula:

$$\bar{S} = \sum_{j=1}^{n} \bar{S}_j \,, \qquad \sigma_S = \sqrt{\sum_{j=1}^{n} \sigma_{S_j}{}^2} \tag{7}$$

In the design based on reliability theory, such limit state as failure of the structure is assumed. This makes it necessary to assess the resistance also in terms of the ultimate strength. Particularly, in case of those members like beams or beams-columns with low slenderness ratio whose resistance is not markedly reduced even when they are deformed by loading exceeding their maximum strength, their resistance must be established with due consideration of their deformation capacity. In this study, the energy that can be absorbed by the member is defined by the strength, using an ideal elasticity model. If the resistance which defines the deformation capacity is expressed as R' and the deformations are taken as θ_1 and θ_2 as shown in Fig. 2, the resistance R^* used in the energy estimation may be given by the following formula:

$$R^* = \sqrt{2\theta_2 \,/\, \theta_1} \cdot R' \tag{8}$$

The load effect S^* can then be obtained from the acting energy W as follows:

$$S^* = \sqrt{2 \cdot W \cdot R' \,/\, \theta_1} \tag{9}$$

By converting R and S into R^* and S^*, the design by means of the energy estimation may be carried out following the same procedure as the design which uses Eq. (6).

3. DESIGN OF STEEL MEMBERS BASED ON RELIABILITY THEORY

Columns and beams are designed by using Formula (6) as described in the preceding section. The statistical values of the respective resistances R_c and R_b which appear in the next section are computed based on the experimental data.

In case of beams-columns, their resistances are governed by two stress conditions; therefore, the method as described above cannot be used for these members. In this report, the design method is presented by expressing the resistance R_{bc} of beam-columns by the following interaction formulas and then by deriving the design standardized value. The resistance R_{bc} and the load effect S may be taken as follows:

$$R_{bc} = \frac{P_r}{p_u} + \frac{M_r}{m_u} = \bar{R}_{bc} \pm K \cdot \sigma_{R_{bc}} \tag{10}$$

$$\left(\frac{M_s}{m_u}, \frac{P_s}{p_u}\right) = \left(\frac{\bar{M}_s}{m_u} + K \cdot \sigma_{\frac{M_s}{m_u}} \cdot \cos\omega, \quad \frac{\bar{P}_s}{p_u} + K \cdot \sigma_{\frac{P_s}{p_u}} \cdot \sin\omega\right) \tag{11}$$

in which P_r and M_r are the existing axial force and the existing moment respectively, p_u and m_u are the nomimal strengths when compressive force only or bending moment only has acted on the members, and ω is the parameter which indicates the state of the load effect. If these two formulas are standardized around the mean value of the load effect, the failure region is converted as shown in Fig. 3. The standardized value at the time of failure can then be obtained from the contact conditions of these two formulas, and consequently the design is carried out by the standardized value given by the following formula:

$$k_f = \left(\bar{R}_{bc} - \frac{\bar{P}_s}{p_u} - \frac{\bar{M}_s}{m_u}\right) \Big/ \left(\sqrt{\sigma_{\frac{P_s}{p_u}}^2 + \sigma_{\frac{M_s}{m_u}}^2} + \sigma_{R_{bc}}\right) > k_d \tag{12}$$

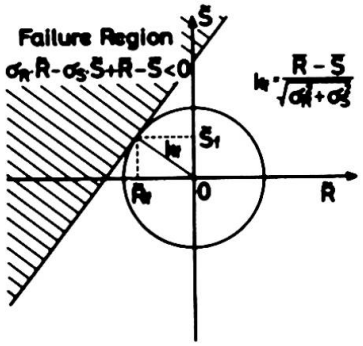

Fig.1 Failure criterion at single stress

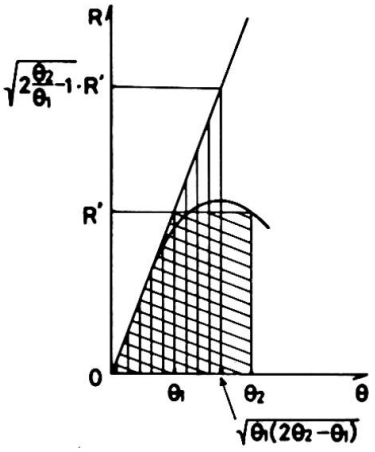

Fig.2 Equivalent resistance

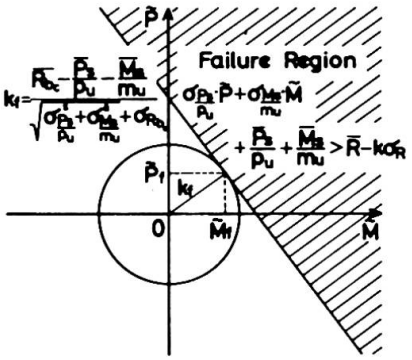

Fig.3 Failure criterion at beam-column

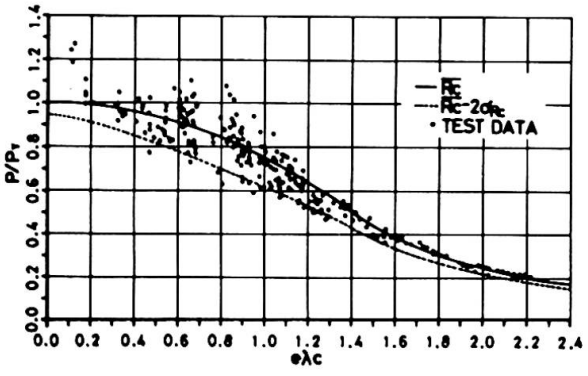

Fig.4 Test data of columns

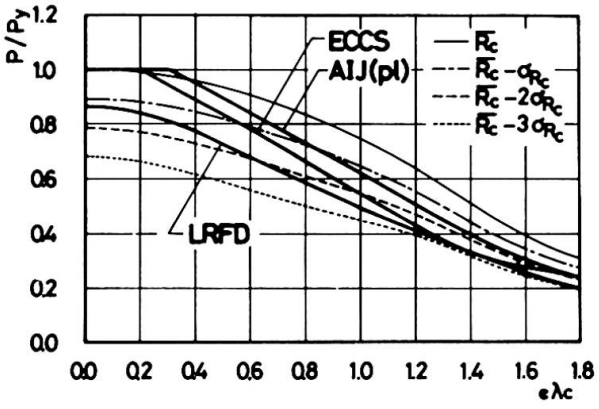

Fig.5 Comparison of mean resistance curves with design column curves

4. MEAN RESISTANCE AND STANDARD DEVIATION OF STEEL MEMBERS

4.1 Resistance of Columns

The statistical values of resistance of columns are obtained by way of the statistical arrangement from the regression analysis results of 270 test data of rolled H-section [4]~[7]. The mean value R_c and standard deviation σ_{Rc} of those values may be formulated as follows. These formulas are devised as means of approximation for practical use, using the equivalent slenderness ratio ${}_e\lambda_c$ (= $1/\pi \cdot \sqrt{Y/e_\ell} \cdot \lambda_y$ in which Y = yield axial force, e_ℓ = Young's modulus and λ_y = slenderness atio for minor axis).

$$0.0 \leqq {}_e\lambda_c < 1.4 \qquad \bar{R}_c = 1-0.25{}_e\lambda_c{}^2 \tag{13-a}$$

$$1.4 \leqq {}_e\lambda_c \qquad \bar{R}_c = 1/{}_e\lambda_c{}^2 \tag{13-b}$$

$$0.0 \leqq {}_e\lambda_c < 0.7 \qquad \sigma_{Rc} = 0.07\exp\{-3.46({}_e\lambda_c-0.7)^2\} \tag{14-a}$$

$$0.7 \leqq {}_e\lambda_c \qquad \sigma_{Rc} = 0.06\exp\{-2({}_e\lambda_c-0.07)^2\}+0.01 \tag{14-b}$$

In Fig. 4, the characteristic values by these formulas are compared with the experimental data. When the correlative variation of yield stress Y and area of cross section A is taken into account, the resistance $R_{c,d}$ and $\sigma_{Rc,d}$ may be expressed as follows, by taking their nominal values as y and a respectively.

$$\bar{R}_{c,d} = \frac{\bar{A}}{a} \cdot \frac{\bar{Y}}{y} \cdot \bar{R}_c \tag{15}$$

$$\sigma_{R_{c,d}} = \frac{\bar{A}}{a} \cdot \frac{\bar{Y}}{y} \cdot \bar{R}_c \cdot \sqrt{\left(\frac{\sigma_A}{\bar{A}}\right)^2 + \left(\frac{\sigma_Y}{\bar{Y}}\right)^2 + \left(\frac{\sigma_{Rc}}{\bar{R}_c}\right)^2} \tag{16}$$

Fig. 5 presents in a comparative way the characteristic strength curves by the two formulae above and the solutions by the present design formula. The design strength in plastic design spec. of AIJ is similar to $\bar{R}_c$ curve in a region of ${}_e\lambda_c \leqq 0.4$ and $\bar{R}_c - 1.8\cdot\sigma_{Rc}$ curve in the elastic region. In elasto-plastic region, the strength is represented by the straight line connecting these two levels. LRFD curve locates between $\bar{R}_c - 2\cdot\sigma_{Rc}$ and $\bar{R}_c - 3\cdot\sigma_{Rc}$ curves. ECCS curve has the intermediate property between AIJ and LRFD curves.

4.2 Resistance of Beams

The statistical values of resistance of beams are obtained, in the same way as for columns, from 223 test data of rolled and welded H-section under uniform moment [8]~[11]. Their R_b and σ_{Rb} may be formulated as follows, using ${}_e\lambda_b$ = $\sqrt{M_p / M_{e\ell}}$ (in which $M_{e\ell}$: elastic lateral buckling moment).

$$0.0 \leqq {}_e\lambda_b < 0.4 \qquad \bar{R}_b = 1.0 \tag{17-a}$$

$$0.4 \leqq {}_e\lambda_b < 1.4 \qquad \bar{R}_b = -0.49{}_e\lambda_b + 1.196 \tag{17-b}$$

$$1.4 \leqq {}_e\lambda_b \qquad \bar{R}_b = 1/{}_e\lambda_b{}^2 \tag{17-c}$$

$$0.0 \leqq {}_e\lambda_b < 0.9 \qquad \sigma_{Rb} = 0.07\exp\{-({}_e\lambda_b-0.9)^2\} \tag{18-a}$$

$$0.9 \leqq {}_e\lambda_b \qquad \sigma_{Rb} = 0.056\exp\{-3({}_e\lambda_b-0.9)^2\}+0.014 \tag{18-b}$$

Fig. 6 indicates on a comparative basis the characteristic values by these formulas and the experimental data. When the randomness of yield stress Y and plastic section modulas Z are taken into account, the resistance $R_{b,d}$ may be expressed as follows, by taking their nominal values as y and z respectively.

$$R_{b,d} = \frac{\bar{Z}}{z} \cdot \frac{\bar{Y}}{y} \cdot \bar{R}_b \tag{19}$$

$$\sigma_{R_{b,d}} = \frac{\bar{Z}}{z} \cdot \frac{\bar{Y}}{y} \cdot \bar{R}_b \cdot \sqrt{\left(\frac{\sigma_Z}{\bar{Z}}\right)^2 + \left(\frac{\sigma_Y}{\bar{Y}}\right)^2 + \left(\frac{\sigma_{Rb}}{\bar{R}_b}\right)^2} \tag{20}$$

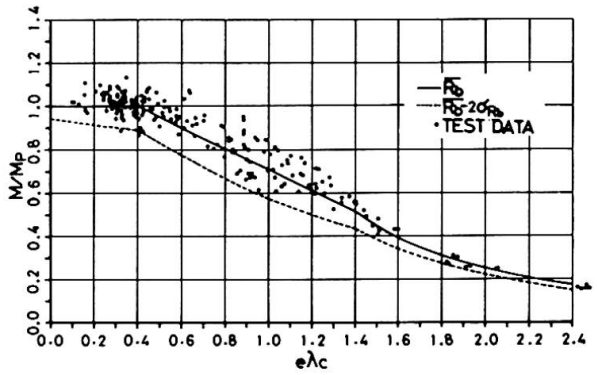

Fig.6 Test data of beams

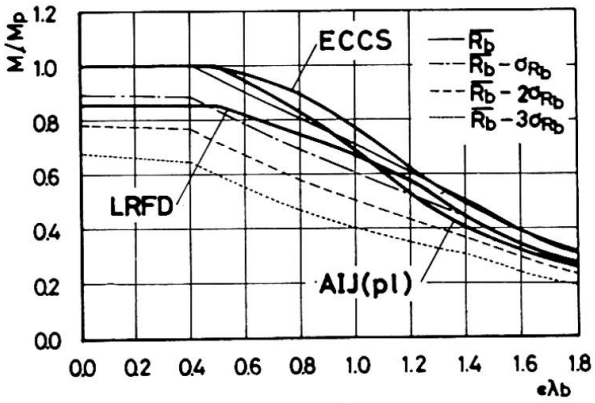

Fig.7 Comparison of mean resistance curves with design beam curves

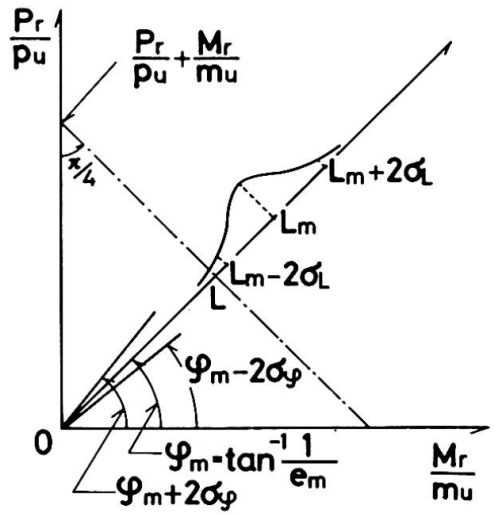

Fig.8 Evaluate method of resistance of beam-column

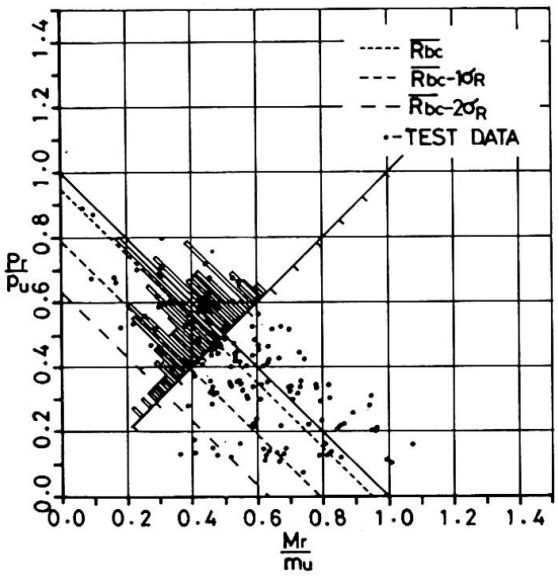

Fig.9 Test data based on Eq.(21)

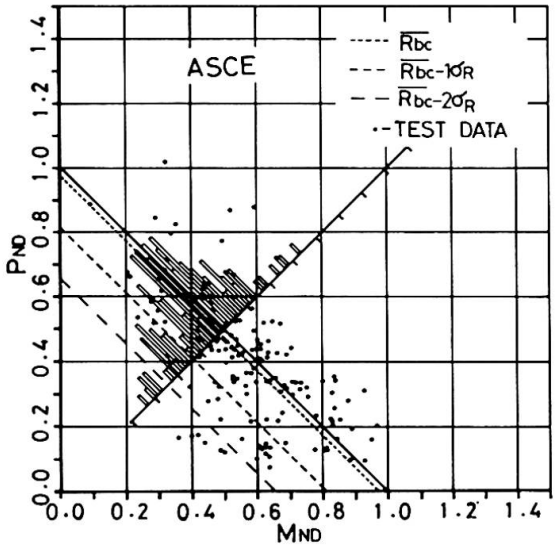

Fig.10 Test data based on ASCE spec.

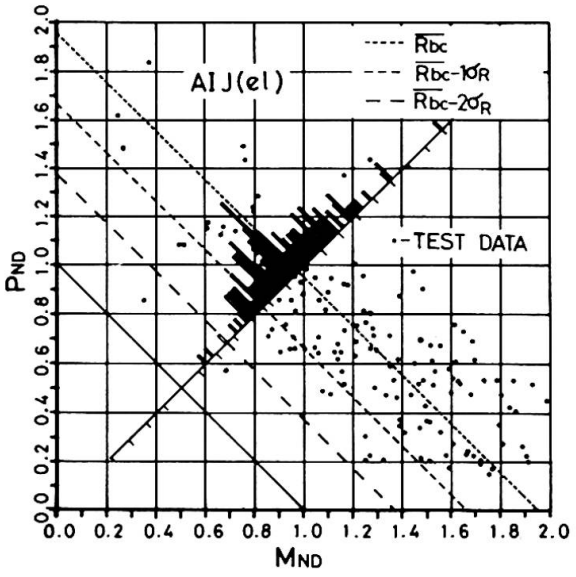

Fig.11 Test data based on AIJ(el) spec.

Fig. 7 presents on a comparative basis the characeristic resistance curves by these formulas and the strength by the present design formula. AIJ(el) and ECCS curves are close to $\overline{R}_b$ curve and LRFD curve is close to $\overline{R}_b - 1 \cdot \sigma_{Rb}$ curve.

4.3 Resistance of Beam-Columns

It is diffecult to formulize the resistance of beam-columns based on regression analysis of test data. In this paper, therefor, the resistance of beam-columns is discussed by test data [12]~[15] which are ploted on the correlogram based on various design formulas. When based on the statistic arrangement method, the resistance is evaluated by making reference to a section of coordinate which consists of the vertical axis presenting the axial force and of the horizontal axis presenting the bending moment (refer to Fig. 8). First, the data is plotted in a coordinate, and then, triangular subsections are selected by lines starting at the origin so that each subsection includes 20 dots of data. Distance of a dot measured from the origin is taken as L. The variation of 20 test data are evaluated in the line which have the mean value $\bar{\psi}$ of an angle ψ as measured from the horizontal axis to each L line. In this case, it is important that the mean value $\overline{R}_{bc}$ and standard deviation σ_{Rbc} of R_{bc} are uniform in every subsections with angle $\bar{\psi}$.

A port of numerical results based on seven design formulas are shown in Figs. 9 to 11. From these results, Eq. (21) is proposed as the best-ballanced form of correlation. The resistance R_{bc} is given with average value of $\overline{R}_{bc}$ and maximum value of σ_{Rbc}.

$$\frac{P_r}{\overline{R}_c \cdot p_y} + \frac{C_m \cdot M_r}{\overline{R}_b \cdot m_p} = 0.95 \pm 0.23K \qquad (21)$$

Where, $C_m = 0.6 + 0.4\beta \geq 0.4$ = moment ratio
p_y and m_p = nominal yield axial force and nominal full plastic moment which correspond to nominal value of p_u and m_u in Eq. (10)
K = standardized value

Fig. 9 indicates the results of this formulas. The data flock a line of average value of 0.95. To illustrate the comparison results of the existing design formulas and test data in the coordinate, Fig. 10 and 11 present the results of ASCE and AIJ(el). In case of ASCE, the average values of data substantially coincide with those of design strength. In case of AIJ(el), the average values of data are two times more distant as compared with the design strength, which fact denotes that two times large marginal allowance is included in the design strength.

5. CONCLUSION

As above, the present study has introduced a design method which is based on the standardized value evaluation. It has been developed with an aim to formulate an approach to the more reliable design system for structural steel members. Also, by the statistical processing of test data, the statistical value of resistance have been formulated, the resulting values being compared with the design formulas now available. The results may be summarized as follows.

The design method, which utilizes the standardized values, consists of two parameters, namely the mean value and standard deviation of the resistance of members and load effects. These parameters directly defines the probability of failure; therefore, designers can incorporate the design level of safety into their design in a numerical way. The statistical values of resistance are calculated by the moment, up to the secondary order, of the mean values and standard deviation from the test data and are resolved into the formula. In this connec-

tion, the resistance based on test data and the design strength according to the design criteria now available are compared. In the succeeding stage, it will be required to make more realistic the statistical values including the load effects for the practicable application of the design method.

REFERENCES

1. A.M. Freudenthal, "The Safety of Structures", Trans. ASCE, Vol. 112, 1947
2. C.A. Cornell, "Sturctural Safety Specifications Based on Second Moment" IABSE Symp. 1969
3. A.M. Hasofer and N.C. Lind, "Exact and Invariant Second-Moment Code Format", Proc., ASCE, EM1, 1974
4. D.K. Feder and G.C. Lee, "Residual Stresses in Hight Strength Steel", Fritz Laboratory Report 269.2, Lehigh Univ., Bethlehem, 1959
5. N. Tebedge, P. Marek and L. Tall, "Comparison of Testing Methods for Heavy Columns", Fritz Laboratory Report 351.2, Lehigh Univ., Bethlehem, 1969
6. N. Tebedge, W.F. Chen and L. Tall, "Experimental Studies on Column Strength of European Heavy Shapes", Fritz Laboratory Report 351.7, Lehigh Univ. Bethlehem, 1972
7. D.H. Hall, "Proposed Steel Column Strength Criteria", Proc. ASCE, ST4, 1981
8. G.C. Lee, and T.V. GaLambos, "Post Buckling Strength of Wide-Flange Beams", Proc. ASCE, EM1, 1962
9. J.F. McDermott, "Plastic Bending of A514 Steel Beams", Proc. ASCE, ST9, 1969
10. T. Suzuki and T. Ono, "Experimental Study of the Inelastic Steel Beam (1), (2),(3),(4)", Trans. of AIJ, No. 168, No.171, No. 175, 1970, No. 202, 1972
11. K. Udagawa, M. Saisho, K. Takanashi and H. Tanaka, "Expemiment on Lateral Buckling of H-Shaped Beams Subjected to Monotonic Loadings", Trans. of AIJ, No. 212, 1973
12. R.C. Van Kuren and T.V. Galambos, "Beam-Column Experiment", Proc. ASCE, ST2, 1964
13. G. Augusti, "Experimental Rotation Capacity of Steel Beam-Columns", Proc. ASCE, ST6, 1964
14. J. Sakamoto and M. Watanabe, "Ultimate Strength of H-Columns under Biaxial Bending (II)", Trans. of AIJ, No. 176, 1970
15. T. Suzuki and T. Ono, "A Study of the Plastic Deformation Capacity of H-Shaped Steel Beam-Column (Part I)", Trans. of AIJ, No. 292, 1980

Effect of Geometric Imperfections on the Design of Steel Box Bridges

Effets d'imperfections géométriques sur la conception des ponts en caisson

Auswirkung Massabweichungen auf die Bemessung von Kastenträgern aus Stahl

Michael S. TROITSKY
Prof. of Civil Eng.
Concordia University
Montreal, Canada

M.S. Troitsky, D.Sc. graduated at the University of Belgrade. A professor of engineering at Concordia University, Montreal. The author of books on "Orthotropic Bridges", "Cable-Stayed Bridges", "Stiffened Plates", "Tubular Steel Structures" and numerous papers on structures.

Eugene THIMMHARDY
McMaster University
Hamilton, Canada

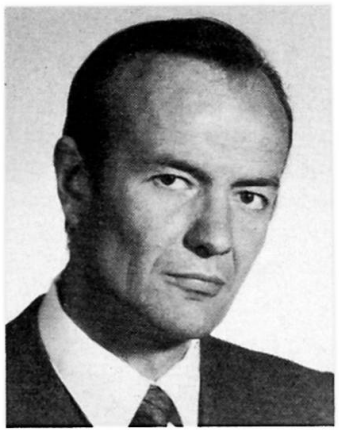

Eugene Thimmhardy, graduated in Railway and Bridge Engineering at the Building Institute, Bucharest. He was principal research engineer in Transport Research Institute, Bucharest, for 14 years, and is now on the staff of McMaster University, Hamilton. His main research interests relate to the behavior of steel bridges.

SUMMARY

Geometric and structural imperfections have unfavorable effects on the ultimate strength of steel-plated structures. To define the magnitude of real imperfections of stiffened plates used in the fabrication of steel box-girder bridges in Canada, a statistical analysis is made of about 10,500 deflection measurements on six in-service bridges.

RESUME

Les imperfections géométriques et structurales ont des effets défavorables sur la résistance ultime des structures en tôles d'acier. Pour définir l'ampleur des véritables imperfections des tôles renforcées, utilisées dans la fabrication des ponts à caisson au Canada, une analyse est faite sur environ 10,500 mesures de déflection sur six ponts en service.

ZUSAMMENFASSUNG

Geometrische und strukturelle Abweichungen haben ungünstige Auswirkungen auf den Bruchwiderstand von Stahlkonstruktionen. Um die Grösse der wahren Messabweichungen von Stahlblechen, die in Kanada für die Herstellung von Hohlkastenträgern benützt werden, zu definieren, wurde eine statistische Analyse von 10'500 Durchbiegungsmessungen an sechs in Betrieb stehenden Brücken durchgeführt.

1. INTRODUCTION

The detrimental effect of structural and geometrical imperfections produced during the fabrication of welded stiffened plate structures on their buckling strength has for a long time been recognized. The measured magnitude of geometric imperfections, as well as those tolerances prescribed by codes, differ rather significantly from one country to another.

With the introduction of the limit states design philosophy which has now been adopted all over the world, it became essential to assess the actual ultimate strength of all elements and more specifically, those of the entire structure. The application of limit states in the design of plated structures implies the use of the semi-probabilistic theory in defining the magnitude of geometric imperfections as well as their correlation with the loss of strength of the structure.

Since 1979, Canada has introduced the limit states method in the design of highway bridges first in the province of Ontario [1] and tends to extend its application to the national level [2]. The uncertainty of the real magnitude of geometric imperfections and their influence on the buckling strength of compression flanges appears to be the main reason for restriction of their applicability to spans up to 50m for steel box bridges [1].

2. GEOMETRIC IMPERFECTIONS OF STEEL BOX BRIDGES IN CANADA

2.1 Measurement Program

To undertake the research program, six in-service steel box bridges across Canada have been chosen. It was anticipated that the average fabricating conditions or significant differences in the value of geometric imperfections from province to province would be evident. The pertinent features of these highway bridges are given in Table 1.

The above bridges were selected because the box girders are of large cross-section, are continuous over interior supports, and have spans longer than 50m. The negative moments which occur over the support regions induce significant compressive stresses in the bottom flanges. Since geometric imperfections are of concern in these areas, the major part of the measurements was concentrated here.

The geometric imperfections referred to in this paper include the out-of-flatness of the web subpanels and bottom flanges (f_1) and out-of-straightness of the longitudinal stiffeners (f_2).

To relate the measurements performed on in-service bridges, i.e., including the effect of their dead loads, with the imperfections produced during fabrication, a small correction should be applied to the former. It is claimed that this correction is likely to be less than 5% [3].

2.2 Results of the Measurements

To establish reliable values of imperfections, the statistical approach is recommended, and in this regard, a large number of measurements are needed. In the study performed, a number of 10,500 measurements were used to define the statistical parameters. Statistical analyses of the data were undertaken for each bridge and their aggregate [4] . As a representative magnitude of these imperfections the 95% fractile that has been extensively employed [3] was adopted. Table 2 defines the mean value, standard deviation and 95% fractile value obtained from the statistical analyses of aggregate data for the six bridges for the out-of-flatness subpanels and out-of-straightness longitudinal stiffeners.

		BRIDGE					
		Drinkwater	Glen Morris	Portage	Muskwa	Campbell	Mission
Spans (m)		69.56+85.34 +60.96	52.73+2@45.72 +59.43	36.58+85.34 +36.58	55.25+2@91.44 +54.86+36.88	2@55.17	88.39+134.11 +88.39
Length (m)		207.26	203.61	158.50	329.87	110.34	310.90
Type of Beams			CONTINUOUS				Cantilever
Number of Box Girders		4	2	5	2	3	1
Cross-Section		TRAPEZOIDAL			RECTANGULAR		
Dept. of Webs		CONSTANT		VARIABLE			
Width of (mm)	Bottom Flanges	1329	1219	Varies (1626-2388)	2591	1575	11252
	Panels	600	445	Varies (406-597)	520	560	675
Fabrication Year		1973	1972	1973	1975	1976	1974
Structural Steel	Specification	CSA G40.11 Grade B	CSA G40.11 Grade B	CSA G40.11 Grade B	CSA G40.21 Grade 50A	CSA G40.21 Grade 50A	CSA G40.8 Grade B
	Min.Yield Strength (MPQ)	250	250	250	350	350	350

Table 1

2.3 Comparison With Specifications

Fabrication tolerances prescribed in existing codes differ greatly from one country to another and they depend upon the experiences, technologies and traditions of the fabricators. Following the recommendations of a Task Group chaired by Professor Ch. Massonnet, a set of more realistic and easy to control tolerances has been proposed [3]. These tolerances which should be applied on unloaded bridges and in the opinion of the Task Group can generally be respected, are:

$f_1/200$ - for the deformation of plate panels, and

$f_2/500$ - for the deformation of longitudinal stiffeners.

It is evident from Table 2 that in the case of those steel box bridges studied in Canada, the measured imperfections of the bottom flanges meet neither the prescribed tolerances [5] accepted in Canada, nor the proposed tolerances mentioned above.

Comparing those values of geometric imperfections defined in Table 2 with those obtained in other countries [3],[10], one can note that they are comparable with those found in West Germany and Czechoslovakia and are larger than those established in Belgium and the United Kingdom. Even those values of geometric imperfections obtained in Canada, West Germany and Czechoslovakia should be decreased by 5% to take into account the influence of dead load; they remain larger than the prescribed tolerances for unloaded bridges. This increase represents about 70% in the case of out-of-flatness subpanels and 35% in the case of out-of-straightness longitudinal stiffeners for bottom flanges with thicknesses less than 30 mm.

3. EFFECT OF IMPERFECTIONS ON THE DESIGN OF STIFFENED COMPRESSION PLATES

3.1 General Considerations

The design of stiffened compression flanges by taking into account the influence of imperfections, can be conducted in one of the two ways developed during the last decade. First, is to treat the stiffened plate as a series of struts and to apply inelastic beam-column methods in assessing their strength. The second is to treat the discretely stiffened flange as a plate assemblage. In the last case, either the modified linear buckling theory or the non-linear post-buckling theory can be applied. [9] Although the second approach has been proposed by many authors, the only ones to appear in the codes under review are the inelastic strut approach and modified linear elastic buckling theory.[11],[12]

The use of more rational inelastic buckling methods in calculating the ultimate limit states could lead to greater consistencies in element strength and existing research information should be used in the new design codes. In the actual transition period from the older elastic based methods to the newer ultimate load ones, even the introduction of an inelastic strut approach in the design codes has to be welcomed. In this regard, the new British Standard [6] and American proposals [5] should be noted.

3.2 Magnitude of Imperfections to be Applied in the Design Analysis

The use of inelastic methods in the design analysis of stiffened compression plates implies the knowledge of magnitude of structural and geometrical imperfections. The values of imperfections to be used in the design codes should reflect the real study of the fabrication industry and they could differ from one country to another. As previously shown, the measured values of imperfections in Canada and in other countries are different from the tolerances prescribed by the codes. These differences are general due to the fact that the code requirements are not always in relation to the possibilities of the workshops. In these conditions the magnitude of those imperfections to be used in

Position of	Number of meas.	Thickness of the Plate (mm)	f_1/b - Absolute Values				Tolerance of code
			Mean	Standard Deviation	95% Fractile	$1/f_{ip}$ (%)	
a. Panel							f_{ip}/b
	2116	9.53	1/266	1/430	1/127	14.38	
	949	11.11	1/331	1/529	1/157	0.00	
WEB	148	12.70	1/446	1/630	1/191	0.00	1/150 [7]
	72	14.29	1/439	1/621	1/188	0.00	1/61 to 1/160 [5]
AGGREGATE WEBS	3205	9.53 & 14.29	1/290	1/452	1/135	7.82	1/200 [3]
	400	9.53	1/248	1/348	1/106	32.99	
	594	12.70	1/263	1/262	1/88	26.87	
	828	15.87	1/331	1/491	1/149	17.47	
	919	17.46 & 19.05	1/466	1/664	1/201	4.74	1/200[5].[3]
	328	22.23	1/396	1/460	1/132	13.80	
BOTTOM	828	25.40	1/441	1/563	1/147	11.03	
FLANGE	520	28.10	1/334	1/267	1/111	18.84	- [7]
	156	38.10	1/729	1/1264	1/354	0.00	
	96	57.15	1/667	1/1126	1/325	0.02	
AGGREGATE BOTTOM FLANGES	4417	9.53 & 28.56	1/351	1/395	1/117	18.71	
	252	38.10 & 57.15	1/704	1/1147	1/336	0.01	
b. Stiffener			f_2/a - Absolute Values				f_{2p}/a
	387	9.53-16	1/674	1/785	1/338	-	
BOTTOM	1479	17.46-30	1/743	1/964	1/417	-	1/500[5].[3]
FLANGE	284	38.10-57.15	1/1871	1/1473	1/731	-	
aggregate	1866	9.53-30	1/709	1/893	1/366	-	- [7]

Table 2 Statistical results of measured deformations (f_1 and f_2)

design analysis should be the values defined for 95% fractile in a statistical analysis of measured imperfections and not those used for the prescribed tolerances. Because from the designer point of view it is easier to refer to prescribed fabrication tolerances, the magnitude of those imperfections to be applied in design analysis (f_{id}) could be expressed as follows:

$$f_{id} = \alpha_i . f_{ip} \tag{1}$$

where: $i = \begin{cases} 1 - \text{for out-of-flatness subpanels} \\ 2 - \text{for out-of-straightness longitudinal stiffeners} \end{cases}$

$$\alpha_i = \gamma_D . f_{i(95\%)} / f_{ip} \geq 1 \tag{2}$$

$$\gamma_D = \begin{cases} 0.95 - \text{for measurements on in-service bridges} \\ 1.00 - \text{for measurements on unloaded bridges.} \end{cases}$$

$$f_{ip} = \begin{cases} b/200 - \text{for } i=1 \\ a/500 - \text{for } i=2 \end{cases} \tag{3}$$

Referring to Table 2, the corresponding values to be used in Canada should be:

$$\alpha_1 = 1.60 \quad \text{and} \quad f_{id} = 1.60\, f_{1p} \tag{3.1}$$

$$\alpha_2 = 1.30 \quad f_{2d} = 1.30\, f_{2p} \tag{3.2}$$

Similar expressions have been found by using measurement results from West Germany and Czechoslovakia.

Only in cases where an agreement between the measured imperfections and prescribed tolerances has been established, as in the case of Belgium and the United Kingdom [3], can the latter be used in design analysis. In all other cases, Equation (1) should be applied.

3.3 Effect of Imperfections on Steel Box Bridges in Canada

Following the definition of the effect of geometrical imperfections on the buckling strength of compression flanges in six box bridges (Table 1), the inelastic strut approach and the well-known Perry strut equation have been applied. For each bridge the ultimate limit load has been defined as: a) the prescribed fabrication tolerances, b) the geometric imperfection defined by Equation (4.2), and c) for "ideal" flanges without imperfections. For the first two cases a) and b), where the imperfections are taken into account, the nominal value of $0.10\ \sigma_y$ generally recommended for compressive residual stresses has been added.

The detrimental effect of structural and geometric imperfections on ultimate limit loads has been defined by the ratio between the difference in the limit loads of compression flanges with imperfections and those without imperfections with respect to the value of limit loads corresponding to "ideal" flanges. The decrease in the ultimate limit loads established for the six bridges are presented in Table 3.

In general one could note the influence of supplementary eccentricity due to the vertical curvature of the bottom flanges on ultimate limit loads. Referring to Table 3, it should be noted that it was the authors' intention to compare these results with those obtained by using some of the existing codes which have introduced the same approach in the design of compression flanges [5],[6]. It was found difficult to make useful comparisons because of differences in the specified tolerances and also in interpreting the intentions of the code writers.

It is hoped that the measurements of residual stresses, as well as the experimental test program in progress at this time, in Canada, will provide the necess-

Bridge	Magnitude of Geometric Imperfections	
	$f_{2p} = a/500$	$f_{2d} = a/385$
Drinkwater	4.23	5.19
Glen Morris	7.49	8.73
Portage	10.71	12.29
Muskwa	9.83	11.87
Campbell	8.65	10.43
Mission	10.07	13.35

Table 3 Decrease of ultimate limit loads due to imperfections (%)

ary information required for the introduction of inelastic buckling methods in the limit states design of steel box bridges and in this country, which for years has had some of the best design codes in the area of bridges.

4. CONCLUSIONS AND RECOMMENDATIONS

1. The weakening effects of manufacturing and erection procedures on the buckling strength of steel plated structures have been recognized for a long time. In the strength of the structure being affected by its imperfections, the design codes should take into account the influence of those tolerances prescribed by fabrication codes, in using a "performance coefficient - α_i". This coefficient should reflect the existing differences between the magnitude of real imperfections and prescribed tolerances. Some proposal regarding the introduction of larger fabrication tolerances should be carefully analysed by taking into account its implication on the cost and safety of the structure.

2. The prescribed tolerances used in the fabrication of steel-plated structures have to reflect the experience, technologies and traditions of those fabricators specific to each country. They generally have to be such that the workshops will be able to respect them by working well without applying specific procedures.

3. Even though the magnitude of actual measured imperfections are greater than those considered "reasonable" and are proposed [5],[3], or prescribed, it is expected that in the near future the existing gap between the two values will be substantially reduced. The understanding of those people involved in the fabrication and control of steel structures of imperfection importance on structureal strength will probably be the most important factor in reducing this gap.

4. Inelastic buckling methods tend to be adopted in more design codes in this transition period to ultimate limit load methods. It is expected that new methods will be introduced in the near future and in Canadian Design Bridge Codes, due to their consistencies, and in this case, they will take into account the specific fabrication conditions existing in this country, as well as Canadian research contribution in this area.

ACKNOWLEDGEMENTS

The measurement program referred to in this paper was financially supported through the Department of Public Works Canada.

NOTATIONS

a - Plate panel or longitudinal stiffener length
b - Plate panel width
t - Plate thickness
f_1 - Out-of-flatness subpanels
f_2 - Out-of-straightness longitudinal stiffeners
f_{1p}, f_{2p} - Prescribed tolerances referred to f_1 and f_2, respectively
f_{1d}, f_{2d} - Magnitude of geometric imeprfections to be used in design analysis
$f_{l(95\%)}$ - Magnitude of geometric imperfections defined for 95% fractile (l=1,2)
α_i - Performance factor (l=1,2)
γ_D - Imperfection correction coefficient due to the application of dead load

REFERENCES

1. Ontario Ministry of Transportation and Communications, Ontario Highway Bridge Design Code, 1979, Volumes I and II.

2. Canadian Standard Association, Design of Highway Bridges, CSA-CAN-S6-M78, Limit States Design Edition of CSA Standard 6 on Highway Bridges, Revisions to Clause 7 Structural Steel, 1982.

3. MASSONNET CH., Tolerances in Steel Plated Structures, IABSE Surveys, S-14/80, IABSE Periodica 3/1980.

4. KOROL R. and THIMMHARDY E., Geometric Imperfections of Steel Box Girder Bridges in Canada. Report submitted to Supply and Services Canada, Public Works Canada (D.S.S. File No. 55 su EN208-1-2863).

5. Proposal Design Specifications for Steel Box Girders, Final Report No. FHWA-TS-80-205, Wolchuk and Mayrbaurl, Consulting Engineers for Federal Highway Administration, Jan. 1980, Washington, D.C.

6. British Standard Institution, Steel, Concrete and Composite Bridges, Part 3, Code of Practice for Design of Steel Bridges, BS 5400: Part 3: 1982.

7. Ontario Ministry of Transportation and Communications, Specification for Structural Steel, MTC Form 906, Jan. 1981.

8. KOROL R. and THIMMHARDY E., Geometric Imperfections of Steel Box Girder Bridges in Canada, Structural Stability Research Council, 3rd International Colloquium on Stability of Metal Structures, May 9-11, 1983, Toronto, Ont., pp.231-251.

9. TROITSKY M. and SALAHUDDIN A., Modified Design of Box Girders by Nonlinear Theory, Canadian Society for Civil Engineers, 1981, CSCE Conference, May 26-27, 1981, Fredericton, N.B.,pp.205-224.

10. DJUBEK J., KARNIKOVA I. and SKALOUD M., Initial Imperfections and Their Effect on the Limit States of the Compression Flanges of Steel Bridges, 3rd International Conference on Structural Safety and Reliability, Thordheim, Norway, June 23-25, 1981.

11. CHATTERJEE S., New Features in the Design of Beams. The Institute of Structural Engineers, Symposium on BS 5400: Part 3-Draft for Public Comment, Code of Practice for the Design of Steel Bridges, Jan. 1980, pp.19-32.

12. DOWLING P.J., Codified Design Methods for Wide Steel Compression Flanges, The Design of Steel Bridges, Edited by Rockey K.C., and Evans H.R., Granada, 1981, pp.303-328.

Structures à barres et modélisation du comportement des assemblages

Modellierung des Verhaltens von Verbindungen in Stabtragwerken

Modelling of the Behaviour of Joints in Structures

André COLSON
Agrégé de Mécanique
Lab. Méc. et Technol.
Cachan, France

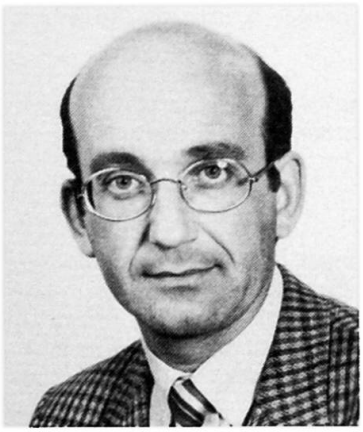

André Colson, 38 ans, enseigne la construction métallique à l'Ecole Normale Supérieure de l'Enseignement Technique depuis 1972 et anime une équipe de recherche sur les assemblages depuis 1977. Il est actuellement Directeur du Département Génie Civil de l'ENSET.

Yvan GALEA
Ingénieur ENSAM
CTICM
Puteaux, France

Yvan Galea, 32 ans, est ingénieur au Département Etudes du CTICM depuis 1975. Chef du service "Etudes et Assistance Construction Métallique", il étudie principalement les problèmes de stabilité et de comportement non linéaire des structures.

Philippe PILVIN
Agrégé de Génie Civil
Lab. Méc. et Technol.
Cachan, France

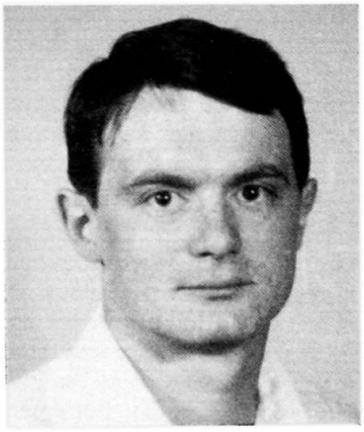

Philippe Pilvin, 26 ans, obtient son agrégation en 1980. Il commence immédiatement une carrière de chercheur au Laboratoire de Mécanique et Technologie.

RESUME

Les codes actuels de calcul des structures postulent l'existence de liaisons parfaites entre les barres. De nombreuses observations expérimentales montrent que cette hypothèse n'est pas réaliste et qu'en fait toutes les liaisons ont un comportement dissipatif non linéaire qui pourrait être mis à profit dans un grand nombre de situations. L'assemblage est modélisé par un macro-élément, doté d'une loi de comportement spécifique, qui est introduit dans un code d'analyse en élasto-plasticité au second ordre géométrique. Des résultats, généralement favorables, sont donnés pour des structures types.

ZUSAMMENFASSUNG

Die heutigen Bemessungsrichtlinien für Stahlbauten setzen das Vorhandensein vollkommener Verbindungen zwischen den Zugstäben voraus. Viele experimentelle Beobachtungen zeigen, dass alle Verbindungen ein dissipatives nicht lineares Verhalten haben, das in zahlreichen Situationen ausgenützt werden könnte. Die Verbindung wird durch ein Makro-Element ersetzt, das ein spezifisches Verhalten hat. Dieses Makro-Element wird einem Computerprogramm für strukturelle Analyse eingegeben, das die geometrischen Effekte zweiter Ordnung und das elastisch-plastische Verhalten des Materials berücksichtigt. Die Ergebnisse werden für typische Strukturen gezeigt und sind im allgemeinen positiv.

SUMMARY

Structural analysis programs, used today, assume a perfect linear behaviour of the connections between the steel elements. A lot of experimental results show that this assumption is wrong. Furthermore, all the connections have a non-linear dissipative behaviour which could be used profitably in many cases. The connection is modelized by a "macro-élément", provided with a specific constitutive equation, which is introduced into a structural analysis computer program which takes into account geometrical second order effects and the material elasto-plastic behaviour. Results are given for typical structure and they are generally positive.

1 – NECESSITE D'UNE ANALYSE REALISTE DU COMPORTEMENT DES LIAISONS

1.1. Modèles habituels de comportement de liaisons

La description topologique d'une structure suppose chronologiquement la connaissance des éléments qui la composent – barres, plaques, coques – et la connaissance de la nature des liaisons entre ces éléments pour préciser les conditions aux limites propres à chacun d'eux. Les modèles habituels de liaisons en mécanique des structures à barres sont :

- l'articulation,
- l'encastrement,
- l'appui élastique.

Cette modélisation par des liaisons parfaites (non dissipatrices d'énergie) est en fait très éloignée de la réalité car les liaisons apparentées à des articulations sont capables d'une rigidité parfois non négligeable tandis que les liaisons apparentées à des encastrements sont susceptibles d'une relative déformabilité. On peut s'étonner d'ailleurs de cette extrême simplification, due à une lacune dans les travaux de recherche, comparativement aux progrès qui ont été réalisés dans le domaine de la connaissance du comportement des matériaux d'une part et dans le domaine du calcul des structures d'autre part.

Dans la conception et le calcul d'une ossature, l'attention de l'ingénieur, au niveau des assemblages, se porte surtout sur les problèmes de dimensionnement des éléments (boulons, soudures, platines) au détriment de l'estimation du comportement global de la liaison.

1.2. Intérêt d'une modélisation « inductive »

La prise en compte d'un comportement global réaliste des liaisons permet d'avoir une meilleure image du comportement effectif d'une structure et notamment la distribution précise des sollicitations. Ceci peut conduire alors à une optimisation interactive lors du choix des barres et des liaisons. L'extrême complexité géométrique d'une zone d'assemblage induit des discontinuités qui ne permettent pas d'utiliser au niveau local les hypothèses classiques de la résistance des matériaux. Les imperfections de fabrication et de montage (contraintes résiduelles, défauts de planéité) contribuent à un comportement complexe de la liaison [4]. Ainsi les discontinuités et les imperfections ne peuvent pas être modélisées une par une selon une méthode déductive qui permettrait par une juxtaposition de comportements élémentaires de remonter à un comportement d'ensemble. Nous proposons à l'inverse une modélisation inductive où l'on considère la zone d'assemblage comme une « boîte noire » gouvernée par une loi entrée-sortie en termes de contraintes et déplacements généralisés qui prend en compte globalement et simultanément l'ensemble des phénomènes qui interviennent dans la liaison.

2 – MODELE INDUCTIF PROPOSE

2.1. Définition du macro-élément assemblage

La « boîte noire » (ou macro-élément assemblage) est située à l'extrémité de l'élément considéré en lieu et place de la zone d'assemblage. Physiquement les dimensions géométriques (figures 1 et 2), sans importance pour le calcul final, sont :

- transversalement équivalentes aux largeur et hauteur de la barre,
- longitudinalement équivalente à la demi-hauteur de la poutre. Cette valeur correspond à la longueur de l'assemblage proprement dit et une toute petite partie de la barre dans laquelle des perturbations importantes dans la distribution des contraintes sont apportées par les éléments d'assemblage. On notera que dans l'utilisation ultérieure cette dimension sera négligeable devant la longueur de la barre.

Les variables retenues pour la modélisation sont celles de la mécanique des milieux curvilignes :

$$- [S] = \begin{bmatrix} N_i \\ \hline M_j \end{bmatrix}$$

$i, j = 1, 2, 3$; N_i et M_j contraintes généralisées (composantes des éléments de réduction des efforts intérieurs) à l'extrémité de la barre.

$$- [\tilde{D}] = \begin{bmatrix} U_i \\ \hline \Omega_j \end{bmatrix}$$

U_i (translations) et Ω_j (rotations) déplacements associés (figure 3) de la section extrémité de l'assemblage par rapport à la section origine.

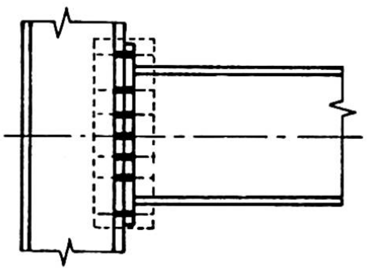

Fig. 1 : Assemblage réel

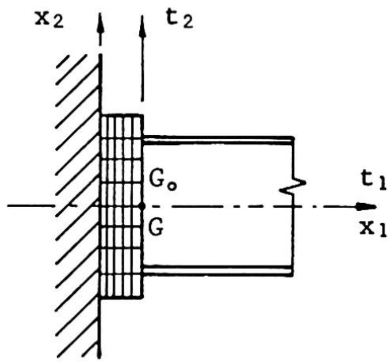

Fig. 2 : Macro-élément équivalent Configuration de référence

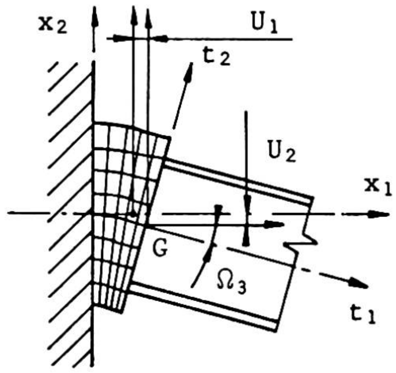

Fig. 3 : Macro-élément en configuration déformée

2.2. Aspects phénoménologiques du comportement

De très nombreux essais ont été réalisés [9] [7], en vue des études de dimensionnement signalés précédemment, que nous interprétons dans le cadre des paramètres et des variables définies pour le macro-élément assemblage. Un résultat type exprimé en loi force-déplacement pour un dispositif expérimental courant est représenté à la figure 4. L'interprétation [4] en terme de contraintes généralisées et déplacements associés est la suivante :

– le comportement est non-linéaire (anélastique) dès le début du chargement,

– la restauration de la rigidité initiale tangente apparaît à chaque inversion du sens de chargement,

– au voisignage de la charge maximale l'évolution du déplacement associé est asymptotique.

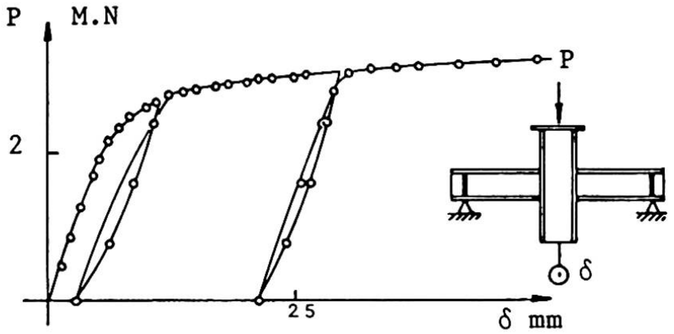

Fig. 4 : Comportement expérimental type.

2.3. Expression du modèle proposé

Dans sa forme générale [10] la formulation incrémentale du modèle fait intervenir une matrice [G] (6 x 6) dont les coefficients sont variables en fonction du niveau du chargement :

$$d\,[\tilde{D}] = [G]\,d\,[S] \qquad (1)$$

Nous utiliserons ici l'expression intégrée de cette loi dans le cas bidimensionnel effort normal-moment fléchissant :

$$U = \frac{N}{K_n}\left(1 + A_n \frac{n}{1-n}\right) \quad \text{avec} \quad n = \frac{N}{N_u}\ ; \qquad (2)$$

$$\Omega = \frac{M}{K_m}\left(1 + A_m \frac{m}{1-m}\right) \quad \text{avec} \quad m = \frac{M}{M_u}\ ; \qquad (3)$$

N_u et M_u sont les sollicitations ultimes d'effort normal et de moment fléchissant (asymptote ou « ouverstress » au sens de [5]).

K_n et K_m sont les raideurs initiales tangentes de l'assemblage pour ces mêmes sollicitations.
A_n et A_m sont les coefficients, constants, qui génèrent la non-linéarité.

3 – PROGRAMME D'ANALYSE NON LINEAIRE

3.1. Principe de l'analyse

Le programme PEP (Programme en Elasto-Plasticité) est un programme d'analyse statique non linéaire en élasto-plasticité des structures planes à barres [6]. Deux effets du second ordre peuvent être pris en compte : l'influence du changement de géométrie de la structure et la perte de rigidité flexionnelle des barres fortement sollicitées axialement. Le programme, basé sur la méthode des déplacements, utilise pour la description du comportement une méthode pas à pas où la matrice de rigidité de la structure est réactualisée en fonction des états de charge, de déplacement, de plastification et de déformation des liaisons. Des analyses simples peuvent être obtenues à moindre coût, sous certaines hypothèses restrictives, mais dans sa forme la plus vaste l'analyse permet de suivre complètement la déformation de la structure jusqu'à la ruine qui peut apparaître [3] :

- soit par formation d'un mécanisme à un degré de liberté dans la structure,
- soit par une perte excessive de rigidité due à un flambement d'élément ou une instabilité globale.

3.2. Expression de la matrice de rigidité tangente [2]

La matrice de rigidité tangente R_T est telle que :

$$[\Delta P] = [R_T]\,[\Delta D] \qquad (4)$$

où $[\Delta P]$ est l'incrément du vecteur charges extérieures et $[\Delta D]$ l'incrément du vecteur déplacement des nœuds. La précision est obtenue en imposant un nombre minimum de pas de calcul. Le macro-élément assemblage est schématisé par deux ressorts à raideur variable en fonction du chargement (figure 5) :

- ressort axial $K_U = dN/dU$
- ressort spiral $K_\Omega = dM/d\Omega$

Les rigidités K_U et $K\Omega$ sont obtenues par inversion des relations (2) et (3) sous forme incrémentale.

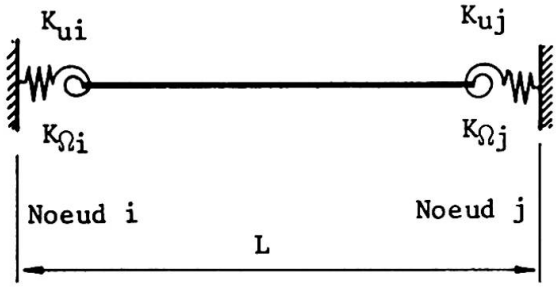

L : longueur de la barre entre points d'épure

I, A : moment quadratique et section de la barre

N : effort normal de compression (< 0)

θ : rotation globale de la barre

Figure 5 : Discrétisation de la barre et des assemblages aux extrémités.

Pour la barre schématisée à la figure 5 la matrice de rigidité tangente $[R_T]$ est donnée ci-dessous :

$$[R_T] = \begin{bmatrix} R_1 & R_1\theta & 0 & -R_1 & -R_1\theta & 0 \\ & R_2 + R_1\theta_2 + \frac{N}{L} & R_4 & -R_1\theta & -(R_2 + R_1\theta_2 + \frac{N}{L}) & -R_4 + LR_2 \\ & & R_3 & 0 & -R_4 & -R_3 + LR_4 \\ \text{(sym)} & & & R_1 & R_1\theta & 0 \\ & & & & R_2 + R_1\theta_2 + \frac{N}{L} & R_4 - LR_2 \\ & & & & & R_3 - 2LR_4 + R_2L^2 \end{bmatrix}$$

avec $R_1 = EA/\gamma L$; $R_2 = (k + \lambda k)\,[2 + (k - \lambda k)\,(1/K_{\Omega i} + 1/K_{\Omega j})] / \alpha\beta L^2$

$R_3 = [k - (\lambda k)^2/\alpha K_{\Omega j}] / \beta$; $R_4 = (k + \lambda k)\,(1 - \lambda k/\alpha K_{\Omega j}) / \beta L$

$\alpha = 1 + k/K_{\Omega j}$; $\beta = 1 + k/K_{\Omega i} - (\lambda k)^2/\alpha K_{\Omega i} K_{\Omega j}$;

$\gamma = 1 + EA/LK_{Uj} + EA/LK_{Uj}$

en compression : $k = (EI/L)\,\eta\,(\sin\eta - \eta\cos\eta) / [2(1-\cos\eta) - \eta\sin\eta]$

$\lambda k = EI/L\,\eta\,(\eta - \sin\eta) / [2(1-\cos\eta) - \eta\sin\eta]$; $\eta = (|N|L^2/EI)^{\frac{1}{2}}$

4 – APPLICATIONS

4.1. Poutre de plancher

Ce premier exemple élémentaire est destiné à montrer le gain sur le poids d'acier à mettre en œuvre qui pourrait être réalisé en modifiant légèrement, par adjonction d'une cornière liant l'aile supérieure, une attache classique assimilée dans les calculs actuels à une articulation. (figure 6).
Dans l'hypothèse d'une articulation à chaque extrémité la charge uniformément répartie ultime est $P_u = 16{,}85$ k N/m. Dans le cas où l'on prend en compte le comportement modélisé des liaisons de la figure 6, la charge ultime est $P_u = 25{,}2$ kN/m, soit une augmentation de 50 % (gain en poids d'acier environ 25 %).

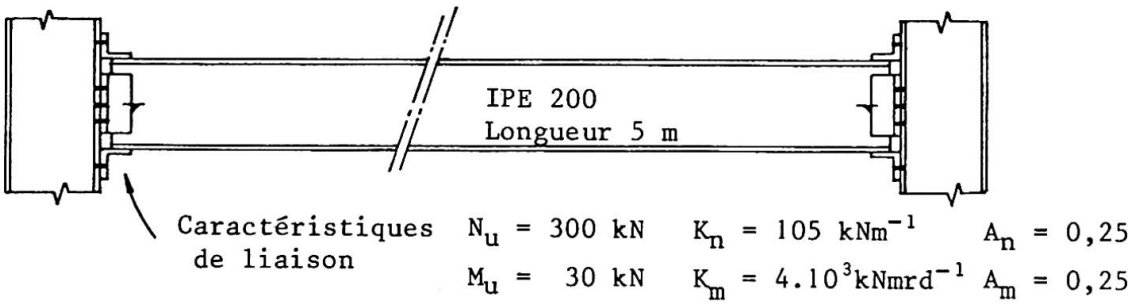

Figure 6 : Caractéristiques géométriques et mécaniques de la poutre.

4.2. Structure à nœuds déplaçables

Afin de mettre en évidence l'augmentation de déformabilité des structures dont la stabilité est assurée par les encastrements des poutres sur les poteaux, par rapport à la modélisation avec encastrements parfaits, nous présentons l'exemple de la figure 7. Deux types de liaisons, dont les paramètres ont été obtenus expérimentalement [1], sont modélisées. Le cas II avec raidisseurs de l'âme du poteau au droit des semelles des poutre et le cas III sans raidisseur. Les déplacements horizontaux calculés pour un facteur de charge de 0,71 (charges de service) sont indiqués à la figure 7. On note une augmentation qui est respectivement de 20 % et presque 100 % dans les cas II et III. Par contre le facteur de charge à la ruine (état limite ultime) n'est diminué respectivement que de 1 % et 18 % par rapport à la solution avec liaisons parfaites.

4.3. Flambement de poteaux

En pieds de poteaux de bâtiment la liaison par platine avec ou sans bêche reposant directement sur le massif de fondation avec boulons d'ancrage, est toujours considérée comme une articulation. Il est évident qu'une telle liaison est en fait susceptible d'une certaine rigidité. Dans le cas d'un poteau HEA240 les caractéristiques de la liaison ont été déterminées à partir d'un modèle d'endommagement du béton au voisinage de la tige d'ancrage [8]. Les résultats sont donnés à la figure 8 en fonction de divers élancements du poteau. Une déformée initiale sinusoïdale d'amplitude maximum égale au 1/250ème de la longueur (courbe b des courbes européennes de flambement) a été prise dans tous les cas. On note l'augmentation de charge à la ruine en fonction de l'élancement (figure 8).

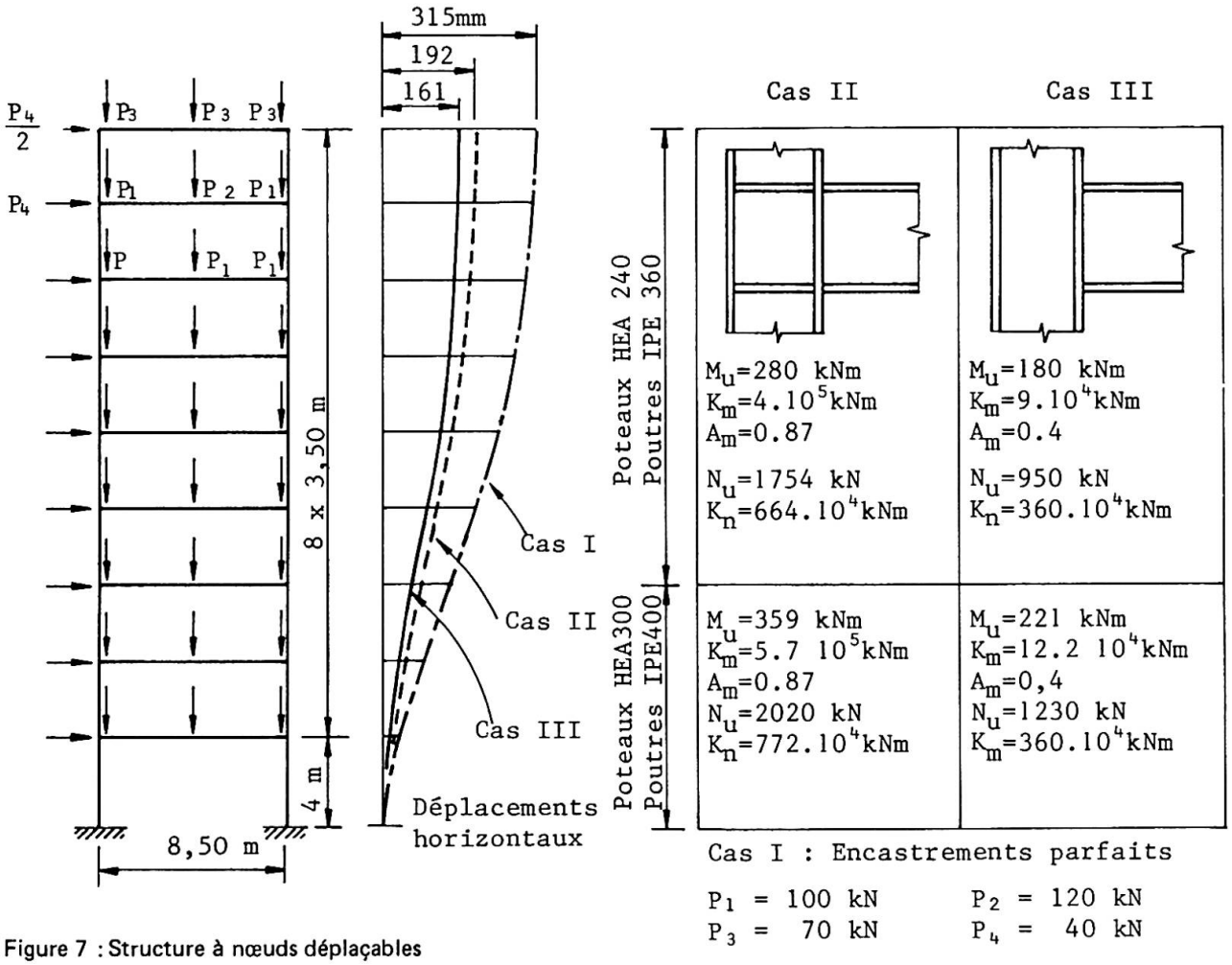

Figure 7 : Structure à nœuds déplaçables

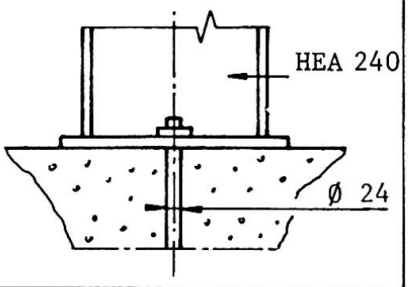

f_0 = 1/250 L

M_u = 32.6 k Nm $\quad N_u = 10^4$kN

$K_m = 15.10^3$k Nm rd^{-1} $\quad K_n = 10^6$k Nm^{-1}

A_m = 1 $\quad A_n$ = 1

Longueur du poteau / Elancement théorique	CHARGE DE RUINE	gain en % par rapport à une liaison parfaite	
	Bi-articulé	1 assemblage 1 articulation	2 assemblages
L = 4 m ; λ = 40	1569 kN	1620 kN (3 %)	1658 kN (6 %)
L = 8 m ; λ = 80	1196 kN	1306 kN (9 %)	1408 kN (18 %)
L = 12m ; λ = 120	784 kN	877 kN (12 %)	975 kN (25 %)
L = 16m ; λ = 160	508 kN	567 kN (12 %)	634 kN (25 %)

Figure 8 : Influence des liaisons aux extrémités sur les charges de flambement

5 – PERSECTIVES

Outre l'intérêt évident d'une meilleure connaissance du comportement d'ensemble des structures métalliques, démontré avec les exemples présentés, en vue notamment du calcul aux états limites, nous pensons que la prise en compte du comportement réel des liaisons peut être profitable :

– en permettant une optimisation des structures par l'utilisation de liaisons semi-rigides, moins onéreuses que les pseudo-encastrements, qui induisent une répartition plus uniforme des sollicitations,

– dans le cas des actions dynamiques (séismes) par le caractère dissipatif des liaisons dû à leur comportement non-linéaire.

BIBLIOGRAPHIE

1. BOUAZIZ J.P., Assemblages poutre-poteau soudés : Dimensionnement et comportement expérimental dans le domaine élastoplastique. Construction Métallique n° 4, pp. 37-50, 1977.

2. COLSON A., GALEA Y., Modélisation du comportement des assemblages. Introduction dans un programme de calcul de structures. Rapports DGRST 82-S-0965, Décembre 1983.

3. COLSON A., GALEA Y., PILVIN P., LESCOUARCH'Y., Programme PEP V d'analyse des structures : Introduction du comportement non linéaire des assemblages. 3ème Colloque international « Stabilité des structures métalliques » Paris, Novembre 1983.

4. COLSON A., Conditions aux limites de liaisons et d'assemblages en mécanique des structures métalliques. Thèse d'État Université PARIS 6, Juin 1984.

5. DAFALIAS Y.F., A novel bounding surface constitutive law for the monotonic and cyclic hardening response of metals. 6th SMIRT, vol. L3/4, Paris, 1981.

6. GALEA Y., Programme d'analyse élastoplastique non linéaire de structures planes à barres. Construction métallique n° 4, pp. 3-16, 1978.

7. JONES S.W., KIRBY P.A., NETHERCOT D.A., The analysis of frames with semi-rigid connections. A state of the Art report, Department of Civil Engineering, University of Sheffield, U.K.

8. MAZARS J., Application de la Mécanique de l'endommagement au comportement non linéaire et à la rupture du béton de structure. Thèse d'Etat Université PARIS 6, Mai 1984.

9. PARFITT J., CHEN W.F., Tests of welded steel beam-to-column moment connection. Journal of the Structural Division, Vol. 102 STI Janvier 1976.

10. PILVIN P., Modélisation du comportement des assemblages de structures à barres. Thèse de 3ème Cycle, Université PARIS 6, Décembre 1983.

Leere Seite
Blank page
Page vide

Ungewollte Schiefstellungen von Stahlstützen

Unavoidable Out-of-plumb of Steel Columns

Position verticale imparfaite de colonnes

Joachim LINDNER
Prof. Dr.
Techn. Univ. Berlin
Berlin

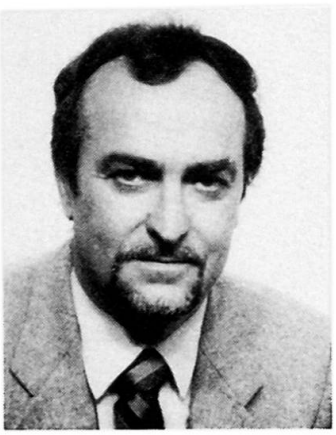

Joachim Lindner, geboren 1938, promovierte während seiner Assistentenzeit 1970 an der TU Berlin. Er arbeitete als Statiker im Stahlbau und später als Abteilungsleiter in einer Gerüstbaufirma. Seit 1974 ist er ordentlicher Professor für Stahlbau an der TU Berlin. Seine Schwerpunkte in der Forschung liegen auf dem Gebiet der Stabilität.

ZUSAMMENFASSUNG
Die aus der ungewollten Schiefstellung von Stützen resultierenden Abtriebskräfte müssen beim Nachweis der Tragsicherheit von Bauwerken berücksichtigt werden. Hier wird über die Auswertung von 725 Messergebnissen an Stützen unterschiedlicher Höhe berichtet. Es wird gezeigt, dass der im Eurocode 3 und DIN 18800, Teil 2 vorgesehene Reduktionsfaktor für grosse Höhen die durch statistische Auswertung ermittelten charakteristischen Werte für die Stützenschiefstellungen gut annähert.

SUMMARY
The fact that columns are unavoidable out-of-plumb results in horizontal forces which must be taken into account in calculating building structures. Here the evaluation of 725 results of measurements is reported. The columns investigated are of different heights. It is shown that the reduction factor of Eurocode 3 and DIN 18800, part 2, gives a good approximation to the statistical characteristic values for the out-of-plumb.

RESUME
Les efforts horizontaux résultant de la position verticale imparfaite de colonnes doivent être pris en compte dans le calcul de structures. L'article interprète les résultats de 725 mesures effectuées sur des colonnes de différentes hauteurs. Il montre que le facteur de réduction de l'Eurocode 3 et DIN 18800, 2ème partie, donne une bonne approximation des valeurs caractéristiques statistiques pour des positions imparfaitement verticales.

1. EINLEITUNG

Beim Tragsicherheitsnachweis von Baukonstruktionen sind in vielen Fällen unplanmäßige, ungewollte Imperfektionen, die aus der Herstellung stammen, zu berücksichtigen. Diese Imperfektionen bestehen i.d.R. aus geometrischen und nichtgeometrischen (sog. strukturellen) Imperfektionen wie z.B. Eigenspannungen. Aus Gründen der Rechenvereinfachung ist es sinnvoll, alle Imperfektionen als geometrischen Ersatzimperfektionen zu berücksichtigen.

Als Grundlage für geometrische Ersatzimperfektionen müssen zunächst die geometrischen Imperfektionen selbst bekannt sein. Diese werden i.a. als Krümmungen w_0 bzw. v_0 von Einzelstäben mit starren Knotenpunkten und Vorverdrehungen ψ_0 von Stützen, Rahmen u.ä., also als Stützenschiefstellungen, auftreten, s. Fig. 1. Rechnerisch können zur Berücksichtigung der Imperfektionen auch Ersatzlasten verwendet werden.

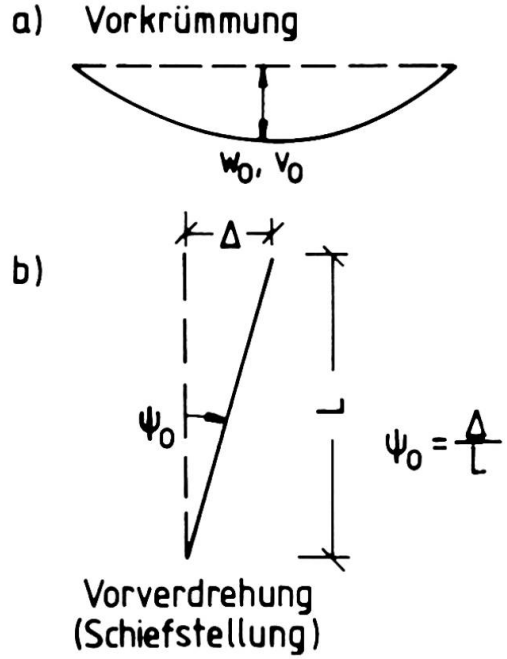

Fig.1 Geometrische Imperfektionen

Der Ansatz von Ersatzlasten oder Imperfektionen, besonders um eine ausreichende Bauwerkssteifigkeit zu erreichen, ist seit längerem bekannt. In Deutschland z.B. durch DIN 1055, Teil 3, Abschn. 7.2 oder DIN 1045, Absch. 15.8.2. Meßwerte liegen diesen Angaben jedoch nur in geringem Umfang zugrunde. In der z.Zt. noch gültigen Norm DIN 4114 (Stabilitätsfälle im Stahlbau) sind Angaben über Außermittigkeiten bei Einzel-Druckstäben, jedoch keine Angaben zu Schiefstellungen von Stützen oder ganzen Tragwerken enthalten.

Für die im Entwurf vorliegenden Normen DIN 18800, Teil 2 [1] und Eurocode 3 [2] sollten daher zusätzliche Unterlagen zur Festlegung rechnerisch anzusetzender Schiefstellungen von Stützen erarbeitet werden. Dazu wurden in Berlin Messungen durchgeführt [3] über die in [4] berichtet wurde. Hier werden weitere Ergebnisse von Messungen an Industriebauten mitgeteilt und zusammen mit den Ergebnissen von [3] ausgewertet. Dabei steht hier die Frage im Mittelpunkt, welchen Einfluß unterschiedliche Stützenlängen (-höhen) haben.

Nach [1] und [2] sind Schiefstellungen wie folgt zu berücksichtigen:

$$\psi = \psi_0 \cdot r_1 \cdot r_2 \qquad (1)$$

ψ_0 Grundwert der Schiefstellung
- = 1/200 wenn beim Nachweis der Tragfähigkeit der Querschnitte das Plastizierungsvermögen ausgenutzt wird
- = 1/300 wenn der Querschnitt höchstens bis zur Streckgrenze beansprucht wird

r_1 Reduktionsfaktor für die Bauteil- bzw. Bauwerkslänge für L>5 m

$$r_1 = \sqrt{5/L\ [m]} \qquad (2)$$

L [m] maßgebende Höhe

r_2 Reduktionsfaktor für mehrere Stützen n in einer Reihe

$$r_2 = 0{,}5(1 + 1/n) \qquad (3)$$

2. MESSUNGEN VON SCHIEFSTELLUNGEN

Nr.	Bauwerk Beschreibung	Anzahl der Messungen	L [m]
1	Hochregallager (Einzelstiele der Gitterstützen)	168	13
	Hochregallager (Einzelstiele der Gitterstützen)	56	39
2	Halle mit Fördereinrichtungen	24	~ 7,5
3	Hochbau (Bibliothek)	32	3,8
	Hochbau (Bibliothek)	15	~ 7,7
4	Zweigelenkrahmen	16	5,0
5	Industriebau (Halle)	18	6,3
6	Rahmen	5	8,8
7	Rohrbrücke (Einzelstiele)	9	~ 3,0
	Rohrbrücke (Einzelstiele)	3	8,5
8	Pendelstütze	3	53,6
9	Kesselhäuser (Einzelstiele)	169	10 bis 20
	Kesselhäuser (Einzelstiele)	64	20 bis 30
	Kesselhäuser (Einzelstiele)	14	70 bis 90
	Kesselhäuser (Einzelstiele)	26	95 bis 125
10	Halle als Kohlebunker	47	13 bis 17
	Halle als Kohlebunker	16	45
11	Maschinenhaus	40	30,7
		Σ 725	

Tabelle 1 Zusammenstellung der untersuchten Bauwerke

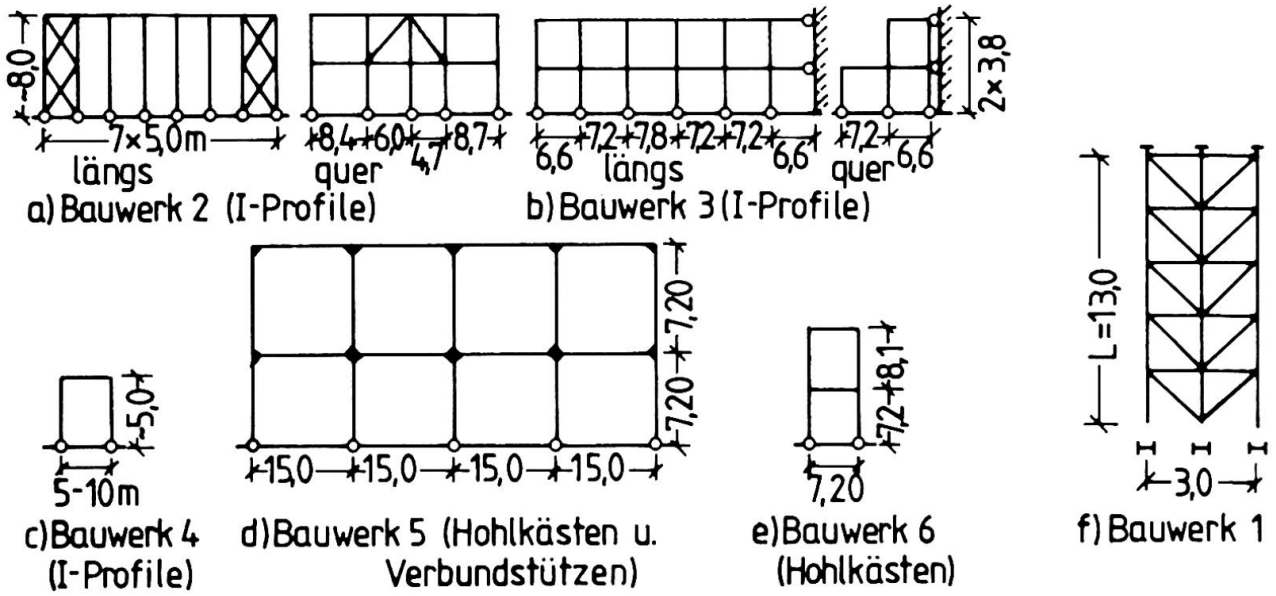

Fig.2 Systeme von einigen untersuchten Bauwerken

Die Messungen wurden an verschiedenen Bauwerken während der Montage, nach dem Ausrichten der Konstruktion und somit bei Beginn des Aufbringens des sonstigen Eigengewichts durchgeführt. Damit sind die Ergebnisse mit guter Näherung als *spannungslose* Vorverformungen zu interpretieren. Hiermit unterscheiden sich diese Messungen von den in [5] beschriebenen, die an Hochhäusern nach dem Aufbringen fast des gesamten Eigengewichts durchgeführt wurden.

Die untersuchten Bauwerke sind in Tabelle 1 zusammengestellt. Dabei wurden unter Nr. 9 acht verschiedene Objekte zusammengefaßt, die alle sehr ähnlich sind. Der Wert L ist jeweils die zu den Meßwerten gehörige Bauteillänge, die in Gl.(2) einzusetzen ist. Die Systeme von einigen Bauwerken sind in Fig.2 angegeben.

Umfangreiche Messungen von Schiefstellungen wurden auch in Kanada durchgeführt, worüber in [5], [6], [7] berichtet wurde. Dabei wurden die Schiefstellungen einzelner Stützen in den einzelnen Geschossen von 2 Hochhäusern (n=2676 Stck.) und die Schiefstellungen der Stützen in einem Industriebau (n=561 Stck.) gemessen. Die Stützenlängen in den Hochhäusern betrugen dabei überwiegend 3,60 m, über die Abmessungen in dem Industriebau liegen keine Angaben vor.

3. AUSWERTUNGEN IM HINBLICK AUF DEN LÄNGENEINFLUSS

3.1 Allgemeines

Die kanadischen Messungen eignen sich nicht zur Untersuchung des Längeneinflusses, da die untersuchten Stützen zu kurz waren (L=3,6 m<5 m). Außerdem sind die Ergebnisse auch nicht auf Gesamtbauwerke zu extrapolieren, da mit der gewählten Meßmethode jeweils die Neigungen der Stützen innerhalb der Geschosse ermittelt wurden, nicht jedoch die Gesamt-Lotabweichungen, in die auch u.a. Stützenversätze und ungenügende Zentrierung der Einzelstützen übereinander eingehen.

Die Meßmethodik bei den in Tabelle 1 zusammengestellten Bauwerken war dagegen so, daß jeweils die Abweichungen Δ von der Lotrechten gemessen wurden, aus denen dann die Vorverdrehungen ψ in Bezug auf die Sehne berechnet wurden. Damit sind alle sonstigen Effekte im Mittel mit erfaßt.

Für die Untersuchung des Längeneinflusses sind auch die unterschiedlichen Bauwerkstypen, unbeschadet event. etwas unterschiedlicher Genauigkeitsanforderungen, gleich gut geeignet. Bei längeren Bauteilen oder Bauwerken erfolgt während bzw. nach der Montage der Einzelteile ein Ausrichten. Damit sind die Schiefstellungen zum großen Teil durch die bei der Montage erreichbaren Absolutwerte Δ bestimmt. Steht ein Stützenteil zu schief nach einer Seite, so wird beim nächsten Teil eine Ausrichtung in entgegengesetzter Richtung erfolgen, so daß auch bei großen Gesamtlängen die Gesamt-Lotabweichungen Δ beschränkt sind.

3.2 Meßergebnisse

Aus Platzgründen können die Einzelergebnisse aller Werte ψ hier nicht mitgeteilt werden, die 349 Werte der Bauwerke 1 bis 8 können [3] entnommen werden. Die Werte des Bauwerkes 10 sind in Tab.2 angegeben. Zur Auswertung wurden die Werte der Schiefstellungen ψ bereichsweise Gruppen zugeordnet. Die Ergebnisse können aus Fig.3 ersehen werden.

Dabei ist zu beachten, daß hier die Absolutwerte der Schiefstellungen ausgewertet wurden. In den Bauwerken ergeben sich die Schiefstellungen sowohl positiv als auch negativ, so daß bei einer genügend großen Zahl von Messungen innerhalb eines Bauwerkes sich der Mittelwert zu Null ergibt und die Verteilung einer Normalverteilung entspricht. Dies wurde auch durch die Messungen in [3] bestätigt, siehe Fig.4a. Wenn man Messungen verschiedener Bauwerke mit einer relativ geringen Anzahl von Messungen vergleicht,ist diese Vorgehensweise nicht möglich, da die Definition positiv/negativ willkürlich vom Meßstandort aus wählbar ist. Die Auftragung kann dann nur über die Absolutwerte erfolgen, was dann zu einer halben Normalverteilung führt, siehe Fig.4b. Diese halbe Normalverteilung ist auch sehr gut aus Fig.3 zu ersehen.

Eine statistische Auswertung der 725 Einzelwerte führt zu folgenden Ergebnissen für ψ:

$$m_1 = 5{,}80 \cdot 10^{-4} \qquad \text{Mittelwert} \qquad (4a)$$

$$s_1 = 7{,}43 \cdot 10^{-4} \qquad \text{Standardabweichung} \qquad (4b)$$

Nr.	L [m]	$\psi \cdot 10^4$	red $\psi \cdot 10^4$	Nr.	L [m]	$\psi \cdot 10^4$	red $\psi \cdot 10^4$
10/1	17	4,12	7,59	10/33	17	0,59	1,08
10/2	17	6,47	11,93	10/34	17	8,24	15,20
10/3	17	1,18	2,17	10/35	17	7,06	13,02
10/4	17	1,18	2,17	10/36	17	7,65	14,10
10/5	13	6,93	11,16	10/37	13	1,54	2,48
10/6	13	6,93	11,16	10/38	13	2,31	3,72
10/7	13	11,53	18,59	10/39	13	0,77	1,24
10/8	13	9,23	14,88	10/40	13	3,08	4,96
10/9	15	3,33	5,77	10/41	15	11,34	19,65
10/10	15	10,66	18,45	10/42	15	3,33	5,77
10/11	15	1,33	2,31	10/43	15	10,66	18,45
10/12	45	0,67	2,0	10/44	15	6,67	11,55
10/13	45	0,44	1,33	10/45	45	3,11	9,34
10/14	45	0,67	2,0	10/46	45	4,89	14,66
10/15	45	1,78	5,33	10/47	45	1,11	3,33
10/16	15	2,67	4,62	10/48	45	4,22	12,67
10/17	17	10,00	18,45	10/49	17	4,12	7,59
10/18	17	9,41	17,36	10/50	17	13,53	24,94
10/19	17	1,18	2,17	10/51	17	2,35	4,34
10/20	17	3,53	6,51	10/52	17	5,88	10,85
10/21	13	3,08	4,96	10/53	13	1,54	2,48
10/22	13	11,53	18,59	10/54	13	15,38	24,81
10/23	13	6,15	9,92	10/55	13	2,31	3,72
10/24	13	6,93	11,16	10/56	15	8,0	13,85
10/25	15	9,34	16,18	10/57	15	3,33	5,77
10/26	15	7,33	12,69	10/58	15	6,67	11,55
10/27	15	8,0	13,85	10/59	15	8,0	13,85
10/28	15	6,0	10,40	10/60	45	1,56	4,67
10/29	45	6,0	17,99	10/61	45	0,44	1,33
10/30	45	2,67	8,0	10/62	45	1,33	4,0
10/31	45	1,33	4,0	10/63	45	4,22	12,67
10/32	45	1,33	4,0				

Tabelle 2

Meßergebnisse von Bauwerk 10 (Absolutwerte)

Diese relativ kleinen Werte sind durch die großen Längen L nach Tab.1 bedingt.

Um festzustellen, ob Gl.(2) eine vernünftige Reduktion darstellt, erfolgt aus diesem Grunde eine zweite statistische Auswertung, indem die Absolutwerte der Meßwerte mit dem Kehrwert der Gl.(2) multipliziert werden (für die Werte mit L > 5 m):

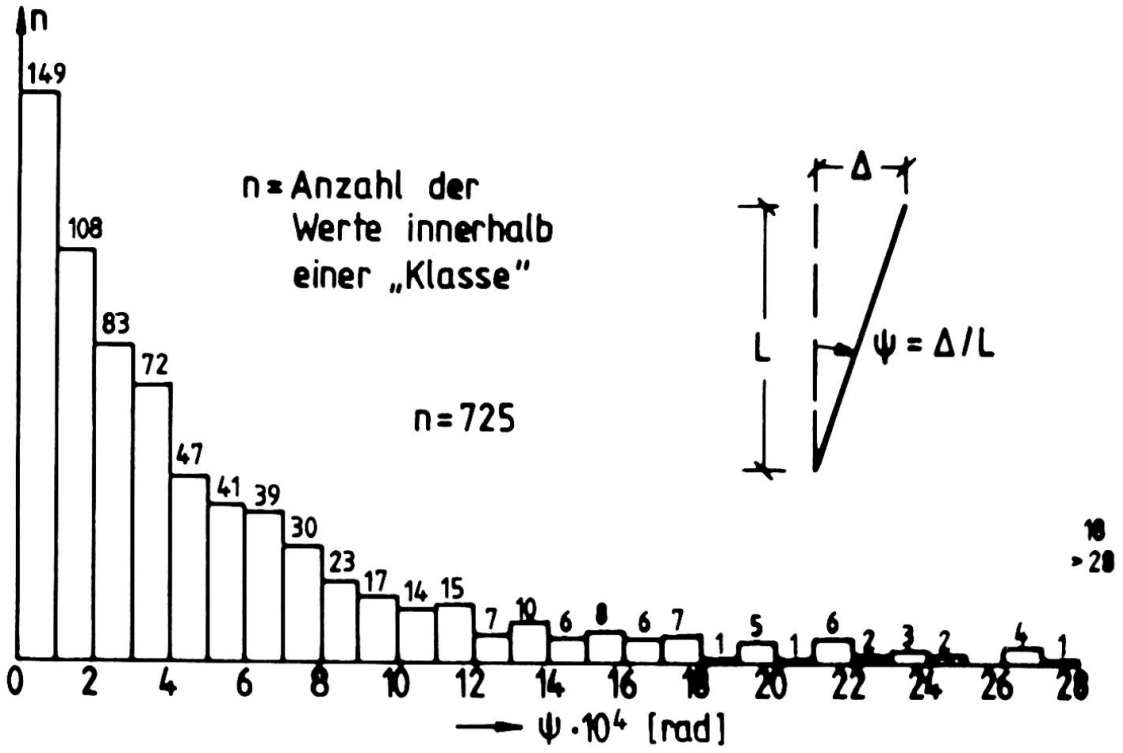

Fig.3 Absolutwerte der Schiefstellungen

$$\text{red } \psi = \psi \cdot \sqrt{L\ [m] / 5} \qquad (5)$$

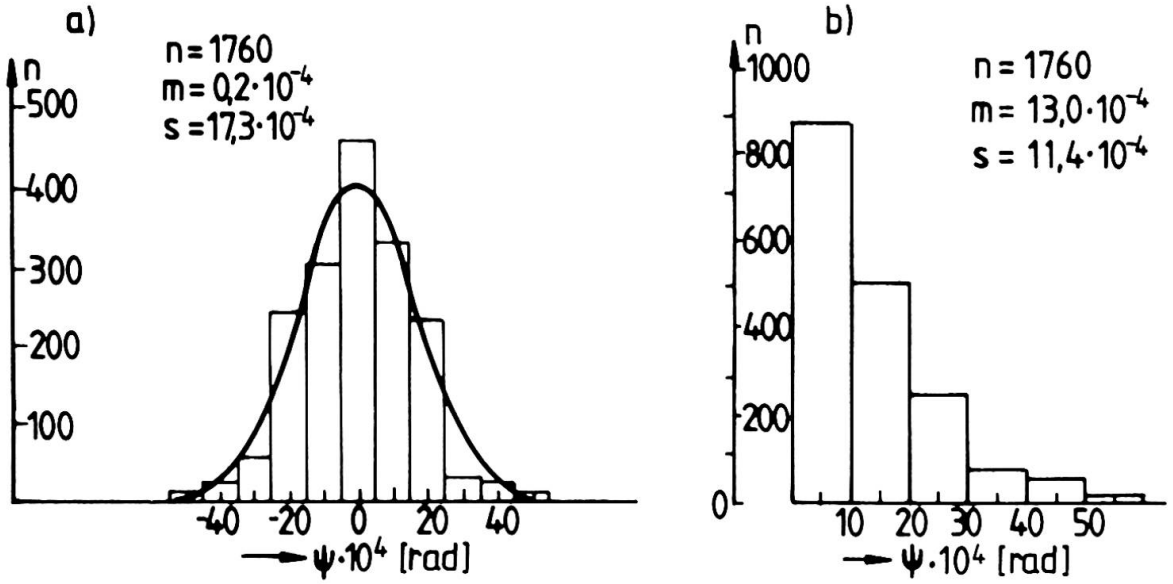

Fig.4 Auswertung der Messungen an einem Hochhaus
a) mit Vorzeichen b) Absolutwerte

Die Ergebnisse sind wiederum in "Klassen" eingeteilt worden und in Fig.5 aufgetragen. Auch hier ergibt sich noch eine angenäherte halbe Normalverteilung.

Eine statistische Auswertung der 725 Einzelwerte führt zu folgenden Ergebnissen für red ψ:

$$m_2 = 9{,}04 \cdot 10^{-4} \qquad \text{Mittelwert} \qquad (6a)$$

$$s_2 = 9{,}16 \cdot 10^{-4} \qquad \text{Standardabweichung} \qquad (6b)$$

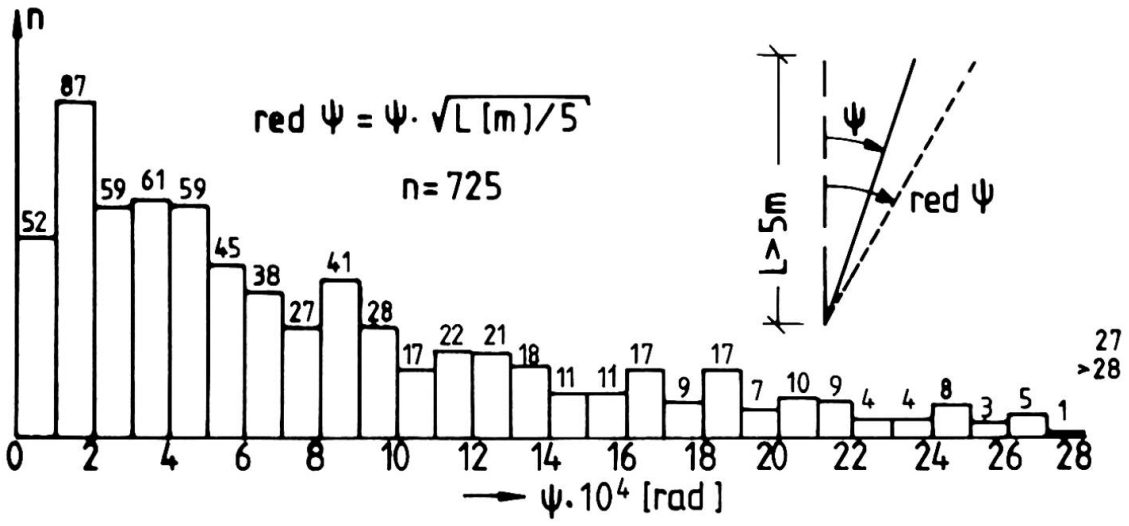

Fig.5 Absolutwerte der reduzierten Schiefstellungen

Wenn (wie z.B. bei den Werten nach DIN 1045 für Betonbauwerke) die 5%-Fraktile zur Ermittlung des charakteristischen Wertes zugrunde gelegt wird, so ergibt sich

$$\text{red } \psi = m_2 + \kappa \cdot s_2 \qquad (7a)$$
$$= (9{,}04 + 1{,}64 \cdot 9{,}16) \cdot 10^{-4}$$

$$\text{red } \psi = 24{,}10 \cdot 10^{-4} = 1/416 \qquad (7b)$$

Dieser Wert stimmt sehr gut mit dem Wert von 1/380 überein, der in [4] zur Bestimmung der in den Normen vorgeschlagenen Ersatzimperfektion ψ_0 benutzt worden ist. In [4] ist auch die Gültigkeit des Reduktionsfaktors r_2 anhand der Auswertung der geeigneten Messungen nachgewiesen worden.

3.3 Einfluß der Auswertung mit Absolutwerten

In [5] sind für die dort durchgeführten Messungen die Auswertungen sowohl unter Verwendung der Meßwerte mit Vorzeichen als auch bei Verwendung von Absolutwerten durchgeführt worden. Die jeweiligen charakteristischen Werte im Sinne der Gl. (7a) sind in Tab.3 angegeben. Aus Spalte 8 ist zu ersehen, daß man mit guter Näherung mit dem Faktor von ca. 0,90 von den Ergebnissen mit Absolutwerten auf die Ergebnisse bei Verwendung vorzeichengerechter Werte schließen kann.

Bauwerk	Werte mit Vorzeichen (Normalverteilung)			Absolutwerte (halbe Normalverteilung)			$\frac{m_1+1{,}64 \cdot s_1}{m_2+1{,}64 \cdot s_2}$
	m_1	s_1	$m_1+1{,}64 \cdot s_1$	m_2	s_2	$m_2+1{,}64 \cdot s_2$	
1	2	3	4	5	6	7	8 = 4/7
A	-0,4	16,2	26,17	11,7	11,2	30,07	0,87
B	0,2	17,3	28,57	13,0	11,4	31,70	0,90
A+B	-0,1	17,0	27,78	12,5	11,5	31,36	0,89
C	1,5	16,0	27,74	11,8	10,8	29,51	0,94

Tabelle 3 Auswertung der Meßergebnisse nach [5]

Wendet man dies an, so erhält man

$$\text{red } \bar{\psi} = 0{,}9 \cdot 24{,}1 \cdot 10^{-4} = 1/461 \qquad (8)$$

4. SCHLUSS

Es werden Messungen von Stützen-Schiefstellungen ausgewertet und es wird gezeigt, daß mit Hilfe des Reduktionsfaktor r_1 die charakteristischen Werte für die Schiefstellungen gut angenähert werden.

LITERATURVERZEICHNIS

1. EDIN 18800, Teil 2, Stabilitätsfälle im Stahlbau - Knicken von Stäben und Stabwerken - Entwurf (12.80) und Arbeitspapier (10.83).

2. Eurocode 3 Stahlbau - Entwurf (1.84).

3. LINDNER J., u. GIETZELT R., Imperfektionen mehrgeschossiger Stahlstützen (Stützenschiefstellungen). Schlußbericht VR 2038A des Instituts für Baukonstruktionen und Festigkeit der TU Berlin zum Forschungsvorhaben IV/1-81/299 des Instituts für Bautechnik Berlin, Berlin, 1983.

4. LINDNER J., u. GIETZELT R., Imperfektionsannahmen für Stützenschiefstellungen. Stahlbau 53(1984), H.4, S.97-101.

5. BEAULIEN D., The destabilizing forces caused by gravity loads acting on initially out-of-plumb members in structures. Ph.D.thesis, Dep.of Civ.Eng., University of Alberta, 1977.

6. BEAULIEN D., u. ADAMS P.F., The results of a survey on structural out-of-plumbs. Canadian Journal of Civ.Eng., Vol.5, no.4, pp.462-470, 1978.

7. BEAULIEN D., u. ADAMS P.F., A statistical approach to the problem of stability related to structural out-of-plumb. Preliminary report to the 2nd Int.Colloquium "Stability of Steel Structures", pp.23-29, Liege, 1977.

New Design Method of Space Structures Using Beam-like Lattice Trusses

Nouvelle conception de structures spatiales, avec des fermes à treillis de type poutrelle

Ein neuer Typ von Raumtragwerken aus Gitterträgern

Toshiro SUZUKI
Professor
Tokyo Inst. of Technology
Tokyo, Japan

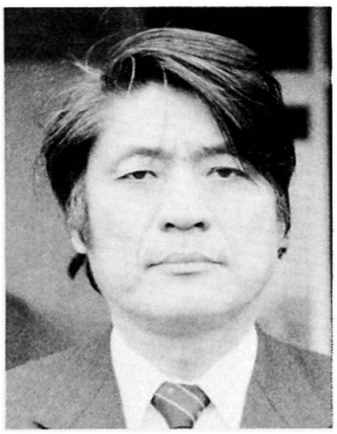

Toshiro Suzuki, born 1936, obtained his doctor of engineering degree at the University of Tokyo, Tokyo, Japan. His major research activities include strength of steel structures, plastic analysis, buckling and ultimate strength of structures, and he is now joint head of the Department of Architecture and Building Engineering.

Toshiyuki OGAWA
Res. Assoc.
Tokyo Inst. of Tech.
Tokyo, Japan

Tooru TAKEUCHI
Grad. Stud.
Tokyo Inst. of Tech.
Tokyo, Japan

Kunio UKAI
Deputy Repr.
Nikken Sekkei Ltd.
Osaka, Japan

Masahiro KATO
Struct. Eng.
Sumitomo Metal Ind.
Tokyo, Japan

SUMMARY

The paper aims at developing a new design method for steel roof structures of large span by using long beams formed of three dimensional trusses. The mechanical properties of these trusses are discussed in terms of experimental results and analyzed by means of continuum theories.

RESUME

L'article présente une nouvelle conception de structures pour des toitures en acier de grandes portées, utilisant de longues poutrelles constituées de fermes à treillis tridimensionnels. Les propriétés mécaniques de ces fermes à treillis sont exposées au moyen de résultats expérimentaux et d'analyses réalisées avec les théories du continuum.

ZUSAMMENFASSUNG

Der Beitrag beschreibt die Entwicklung einer neuen Dachkonstruktion für grosse Spannweiten durch die Verwendung von Raumfachwerkträgern. Die Festigkeitseigenschaften der Fachwerkträger werden anhand experimenteller Ergebnisse diskutiert und mit der Kontinuumstheorie analysiert.

1. INTRODUCTION

At present, convenient and popular structures for covering the roofs with large spans are plane lattice trusses or space frames. As a method contraty to this, we develop a new design method of roof structures using long beams constituted with three dimensional trusses (beam-like lattice trusses) in one direction. The abstract model of beam-like lattice trusses are shown in Fig.1.

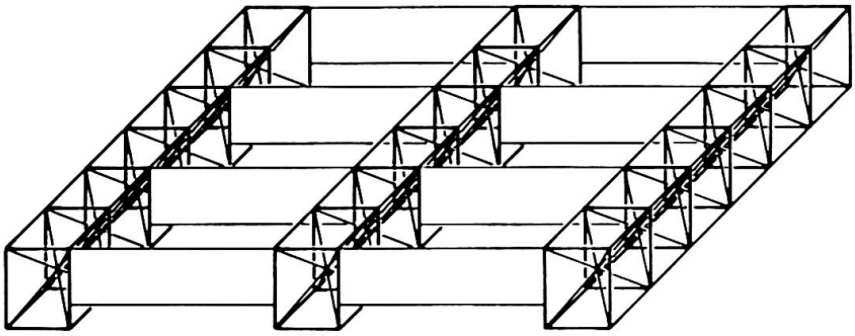

Fig. 1 Wide-span structures using beam-like lattice trusses

The design method of roof structures by beam-like lattice trusses has the following merits.

- -Beam-like lattice trusses have higher strength for lateral buckling as a beam than plane lattice trusses. So they can cover a very large span without lateral restriction.
- -This type of structure is quite simple in dynamics because whole structure has the form of simple beam. Complicated analysis as for space frames is not required.
- -It is superior in productivity and constructiveness because the structural elements are clearly separated. It is easy to arrange for irregular plans for the same reason.
- -This design can be ecconomic and good in shape by arranging the truss members of the beam effectively.

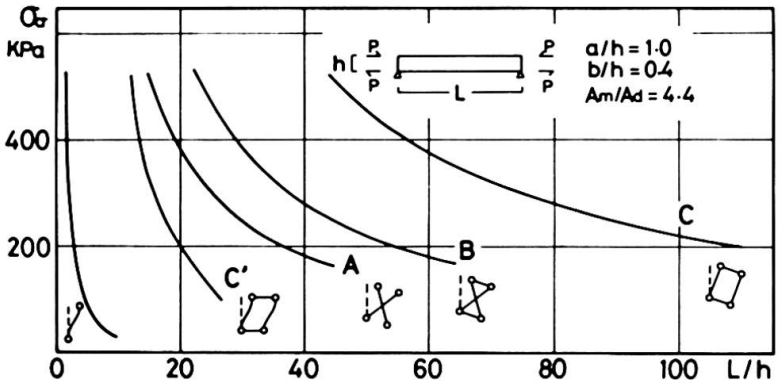

Fig. 2 Lateral buckling strength of lattice beams

The relationship of lateral buckling strength and span of these beams under pure bending are shown in Fig. 2. The lowest curve is that of plane lattice truss, and curves A, B and C are those of beam-like lattice trusses. As is evident from Fig.2, these beams are much stronger for lateral buckling in comparison with plane lattice truss.

In designing this beam-like lattice trusses, the design method of plane lattice can be applied in general, but the design of web members is an exception. In designing web members of plane lattices, only shearing is considered. But, not only bending but torsion act on these beams when vertical load works on one side of the beam, or shear load works on the whole structures by earthquake and wind. Especially, the deflection and the strength of the beam is affected remarkably by torsional load when the beam becomes long. So the design of web members considering shearing and torsion is indispensable in designing beam-like lattices.
In the present paper, for these reasons, we try to comprehend the characters of beam-like lattice trusses under shearing and torsion, and develop the effective design method of web members. This study consists of the following items.

-Design philosophy of the model beams.
-Character of the beams under torsion.
-Character of the beams under shearing and torsion.
-Effective design method of web members.

2. DESIGN PHILOSOPHY OF THE MODEL BEAMS

We set up three type of beams shown in Fig. 3 as definite model to make clear the effect of web members. The design philosophy of these beams are described as follows.

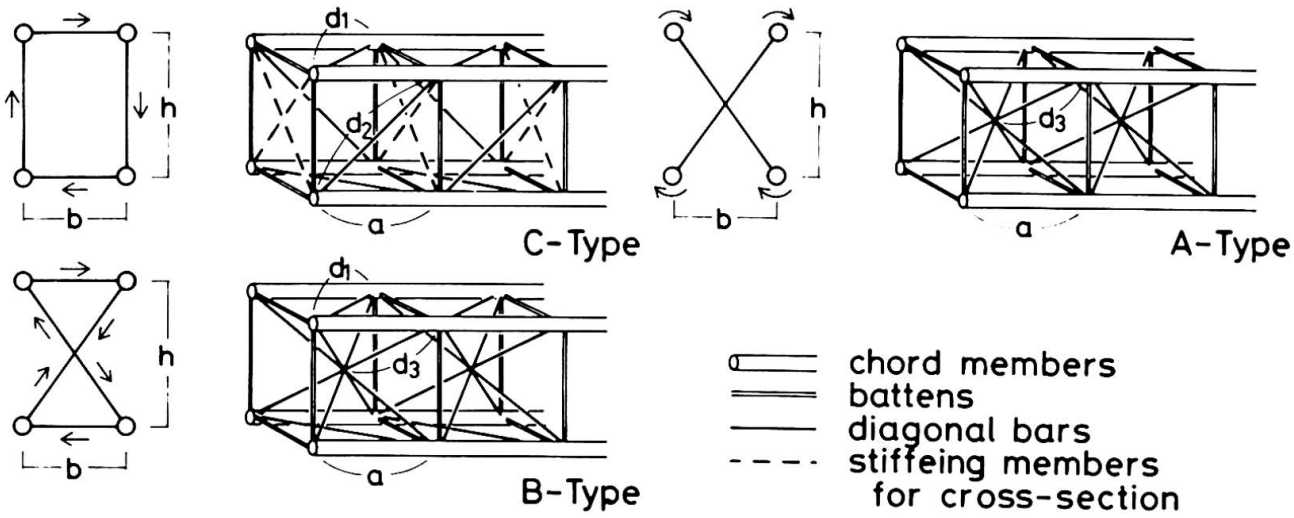

Fig. 3 Models of lattice beams composed of several members

The beam of C-type is the box-section, and has the form of two plane truss beams laced by level diagonal bars. Though these beams are generally designed as only two abreast plane beams against torsional load, the level diagonal bars can be made best use of by stiffening cross-section with cross diagonals and unite the whole beam.
The beam of B-type is trying to save the members by concentrating the vertical diagonal bars to the center of each bay, and serving both as a vertical web members and a stiffening members for cross-section. In addition, it is trying to raise the shearing strength of the whole beam by shortening the buckling length of the web members.
As for the beam of A-type, the level diagonal bars are removed from B-type, and the concentrating diagonal bars resist all directional shearing. The number of the bars of this type is about 1/3 of those of box-section which has the same shearing stiffness in all direction.

3. CHARACTERS OF THE BEAMS UNDER TORSION

3.1 Comprehension by the continuum theory

At first, characters of these model beams under only torsion are discussed.The torsional characters of these trusses are explained by the continuum theory as follows. The beams of C-type and B-type correspond to the closed section, and the axial forces of the diagonal bars resist the torsional moment as shear flow. On the other hand, the beams of A-type correspond to the open section, and the torsional rigidity of the whole beam owes to that of each chord members. From this an idea comes into being that the torsinal rigidity of the beam can be insored by using the chord members which have high rigidity in themselves. From this, the design using steel tubes for chord member will be effective in this type. Because of the difference of axial force distribution, the collapse form of closed section under torsion is expected to be different from that of open section, too. The beams of closed section, as for C-type and B-type, are expected to collapse with rupture or buckling of the diagonal bars. The beams of open section, on the other hand, are expected to break with torsional failure of the chord members, or with bending failure of the web members. The torsional strength of these beams are obtained from the continuum theories.

3.2 Model experiments

We carried out model experiments under torsion on three kinds of the beams of type A, B, C. The specimens consist of the following factors.
All specimens consist of three bays of the beams.
The specimens are fixed at on side with no warping, and torsional moment are caused to act on the other side with the condition free to warp.
All speciments are made up with steel tubes. Chord members are straight and diagonal bars are connected with chord members with welded joint.
The view of the experiment is shown in Fig. 4.

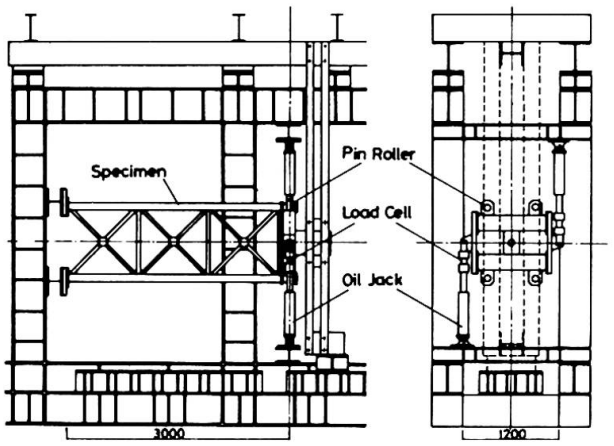

Fig. 4 Set-up of model experiment under torsion

Besides this experiment, the stress distribution and the deflection of these beams under torsion are analized with the finite element method (F.E.M.). The characters of these beams under torsion made clear by the continuum theory, the experiments, and the F.E.M. analysis are discussed as described later. The relationship of load-deflection given by this experiment and the continuum theory are shown in Fig. 5. In them, loads, torsional moment, are given by the product of the breadth and the shear strength of the beam, and deflections, angle of torsion, are given by the breadth. The beam of C-type and B-type broke with the rupture of the diagonal bars shown with the mark "▽" in the figures. Contrary to this, the beam of A-type collapsed with bending yield of the battens and has conspicuously different load-deflection curve from that of B-type which is the beam added diagonal bars on upside and downside to A-type.

The distributions of axial forces of the members of these beams under the unit torsional moment given by the experiment, the F.E.M. analysis, and the continuum theory are shown in Fig. 6. They give the relationships of axial force of the diagonal members and the distance from the fixed end of the beam. As is evident from this figure, the beams of C-type and B-type, the closed sections, resist the torsional moment with axial froces of the diagonal bars and contrary to this, little axial forces generated on A-type, the open section.

From the results described above, it became evident that the stress distribution and the form of collapse of beam-like trusses under torsion is conpicuously different between the closed section and the open section, and these characters are explained exactly by the continuum theory.

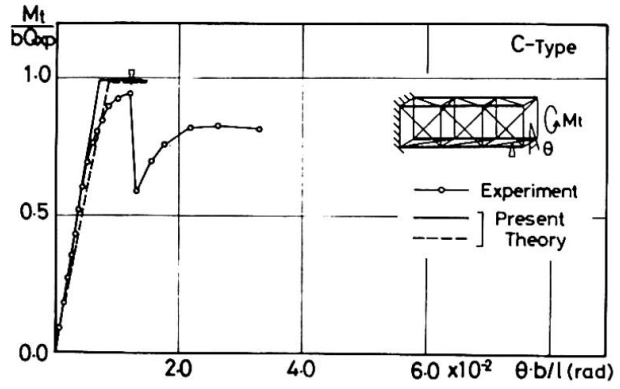

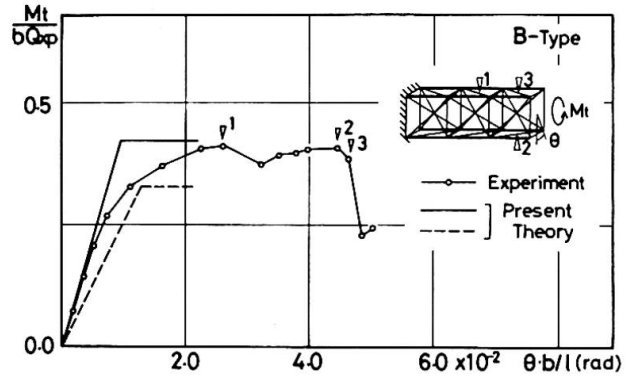

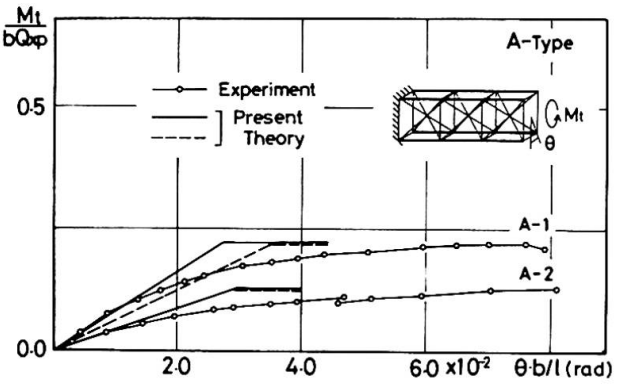

Fig. 5 Torsional moment v.s. torsional angle relationship

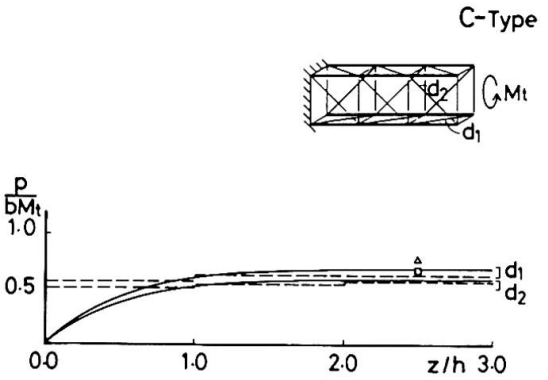

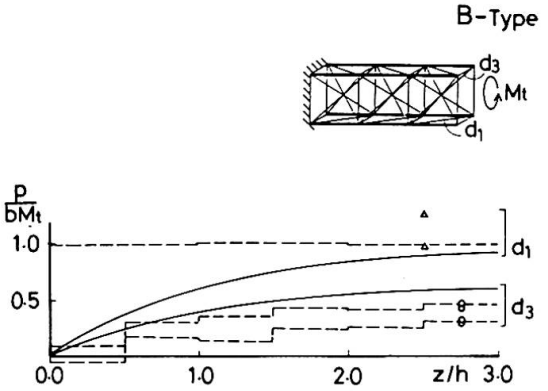

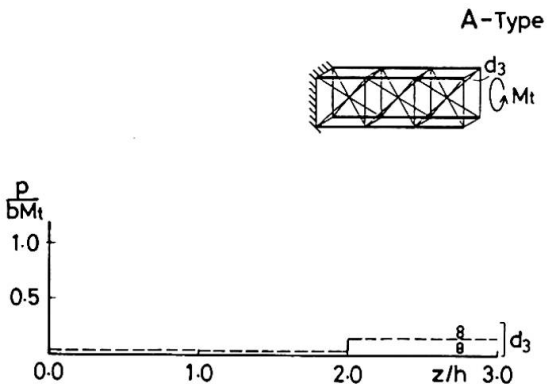

Fig. 6 Axial forces on diagonal members

4. CHARACTERS OF THE BEAMS UNDER SHEARING AND TORSION

4.1 Comprehension by the continuum theory

In this section, we discuss the characters of beam-like lattice trusses under shearing in addition to torsion. This problem is typified by that of the beam under eccentric load, as in Fig. 7.

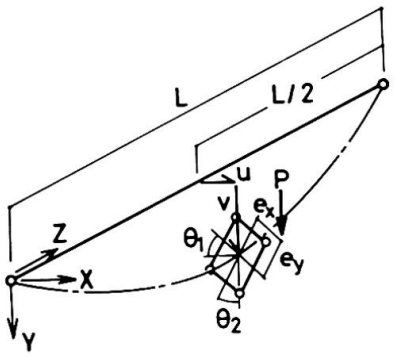

Fig. 7 Lattice beam under eccentric load

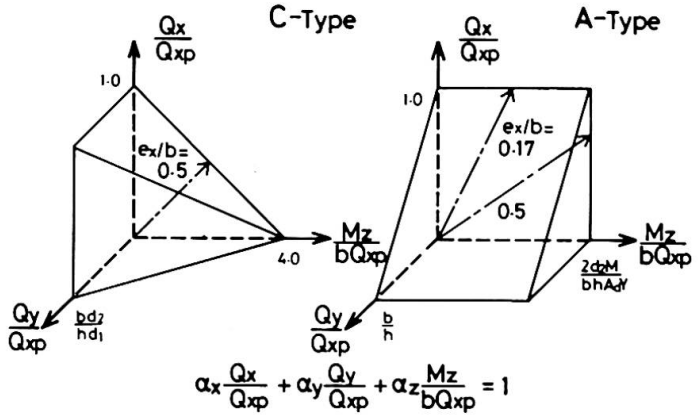

Fig. 8 Failure criteria of lattice beams

We selected the beam of C-type and A-type as specimens, which are typical as closed section and open section respectively. The failure criteria of C-type and A-type are shown in Fig. 8. Qx, Qy, Mz mean respectively shearing loads with respect to strong axis, shearing loads with respect to weak axis, and torsional moment, and each axis is given by the shearing strength with respect to the strong axis without eccentricity. This figure means that the beams collapse when the condition of loads reach these surfices. As for C-type, the closed section, the strength under shearing loads and that of torsional moment interacts each other because the torsional moment produces axial forces on diagonal bars which resist the shearing loads. Contrary to this, as for A-type, the open section, the strength under these loads are indepent because no axial forces are produced in the diagonal bars by torsional moment.
The path of loads condition under eccentnic bending load are shown in the figures.

4.2 Model experiments

We carried out model experiments under torsion and bending on two kinds of the beams, A-type and C-type. The specimens consist of the following factors.

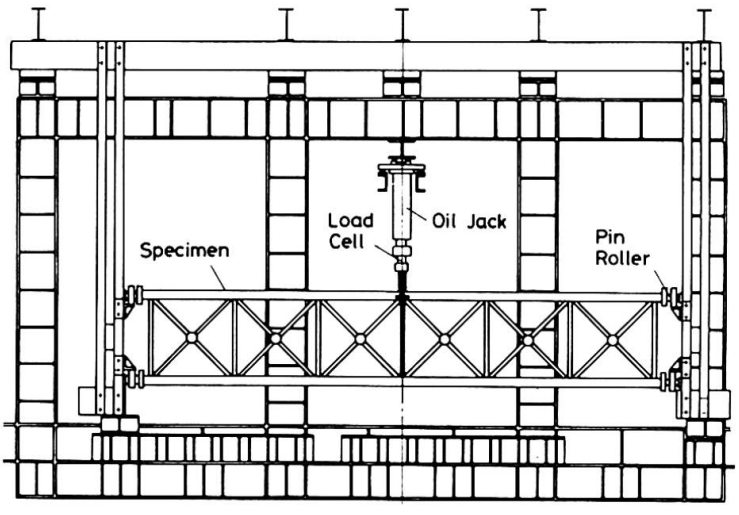

Fig. 9 Set-up of model experiment under torsion and bending

-All specimens consist of six bays of the beams. Their construction are equal to those of the experiments of torsion, described in 2.2.
-The specimens are simple-supported and eccentric loads are applied on the center of these beams. The load points are free to move horizontally according to the revolution of the section of the beams.

The view of the experiment is shown in Fig. 9.

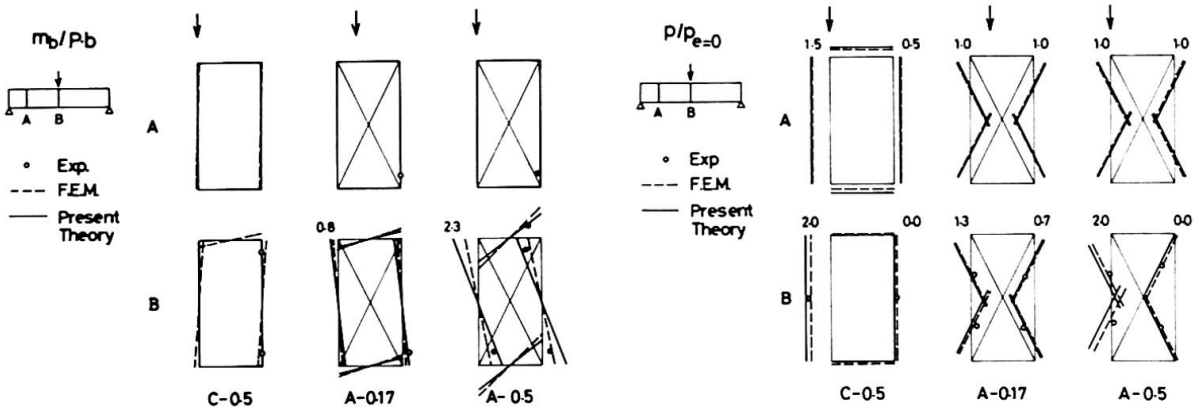

Fig. 10 Axial forces on diagonal members

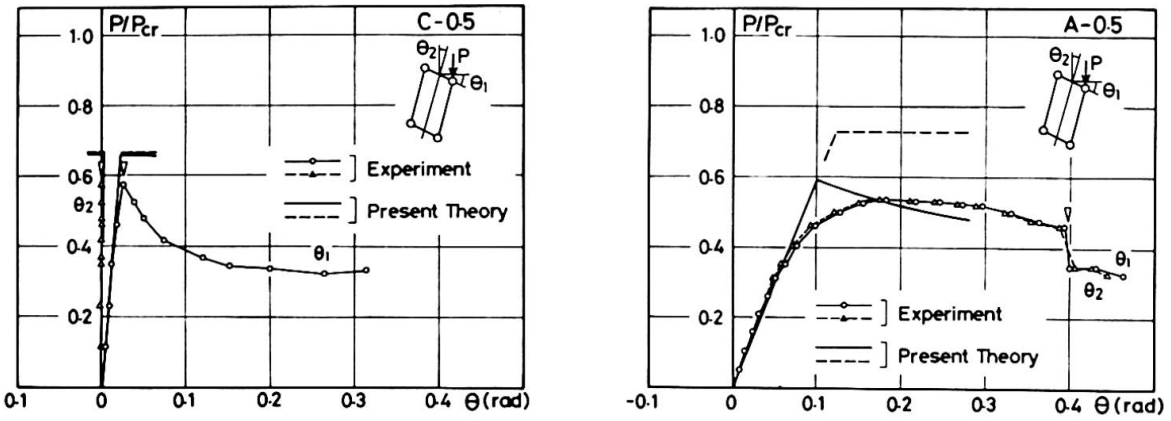

Fig. 11 Concentrated load v.s. rotation of central section relationship

The stress distributions of the diagonal bars of theses beams under the unit eccentric load obtained by the experiment, the F.E.M. analysis, and the continuum theory are shown in Fig. 10. The figure shows axial forces of the diagonal bars and bending moments of the battens, severally at the center and the section at intervals of two bays from the center. What is evident from these figures is that the reaction against bending and torsion are devided severally by the diagonal bars and the battens in the open A-type, contrary with the closed section C-type, in which both bending and torsion are born by the diagonal bars.

The relationships of load-rotation of central section obtained by this experiment and the continuum theory are partially shown in Fig. 11. In them, loads are given by the shearing strength of the beam with no eccentricity. The beam of C-type broke with the buckling of the diagonal bars and the load falls rapidly. Contrary to this, A-type under the same condition broke with the bearing yield of the battens and had superior deformation capacity, which is important in the earthquake and wind resistant design. Adding to this, A-type has the strength almost equal to C-type under bending and torsion though it is inferior under torsion only. These characters are because of the wide distribution of the stresses, and they can be considered as common characters to the open section. The final view of the experiment is shown in Photo. 1.

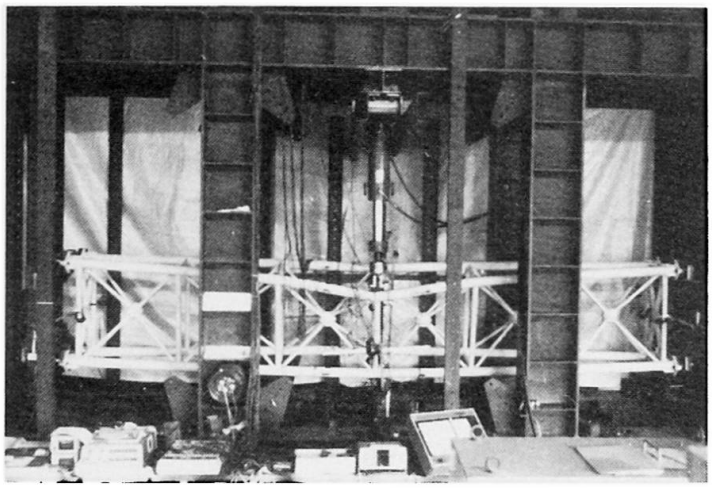

Photo. 1 Final view of specimen

5. EFFECTIVE DESIGN OF THE BEAM

Special merits of the steel roof structures by beam-like lattice trusses and the mechanical properties of these beams are discussed. By using these results, effective design for large span can be developed. For example the beam of A-type, set up in this study, is proved to have excellent characters as follows.

- -Diagonal bars concentrating to the center of each bays resist all directional shearing, and number of the diagonal bars of this type is saved to about 1/3 of those of box-section which has the same shearing stiffness in all direction.
- -This type of beam has a good appearance because of the radial bars in its each bays.
- -The torsional rigidity of whole beam is insored by using steel tubes for chord members.
- -Because of the wide distribution of the stresses, the strength of this type under shearing and torsion is not inferior to that of box-section inspite of saving members.
- -A beam of this type has superior deformation capacity when it collapses with bending yield of battens. This cahracter is important in the earthquake and wind resistant design.
- -For the case where high torsinal rigidity should be needed, this type can easily cope with the situation by adding diagonal bars on its upside and downside and changing it into B-type.

REFERENCES

1. NAN S.S., Torsional Analysis for Suspension Bridges. Proc. of ASCE, Vol.83, No. ST6, 1957.
2. S.KOMATSU and N.NISHIMURA, Three Dimensional Analysis of Truss Girders by the Thin Walled Elastic Beam Theory. JSCE, No.238, June, 1975.
3. A.K.NOOR and C.M.ANDERSON, Analysis of Beam-Like Lattice Trusses. Computer Methods in Applied Mechanics and Engineering, 20, 1979.
4. T.SUZUKI and M.KIMURA, Behavior of Steel Beams under Eccentric Lateral Load. Transactions of Arckitectural Institute of Japan, May, 1976.
5. T.SUZUKI and T.TAKEUCHI, Tortional and Lateral Buckling of Three-Dimensional Truss Beams. Summaries of Technical Papers at 1983 Annual Meeting of Archt. Inst. Japan.

Conclusions au Séminaire V
Développement dans le projet et le calcul de constructions métalliques

Jean-Claude BADOUX
Professeur
Ecole Polytechnique Fédérale
Lausanne, Suisse

Les bases de calcul des charpentes métalliques sont très uniformes à travers le monde. L'important effort entrepris depuis quarante ans en recherche fondamentale et appliquée est parfaitement international. Il a porté de très nombreux fruits et a contribué puissamment à développer favorablement les règles de calcul, à les uniformiser également.

Plusieurs des contributions présentaient des résultats intéressants de recherches et de développements récents. Devant la grande masse de recherches théoriques, il est des plus intéressants de connaître des résultats de recherches prenant en compte la réalité physique de constructions réelles.

Ce furent en particulier les contributions des Professeurs O. Halasz (H) et J. Lindner (RFA) sur la réalité des comportements à la ruine et la non-verticalité de colonnes qui allèrent dans cette direction.

Leere Seite
Blank page
Page vide